

SCIENTIFIC REPORTS

OPEN

Mutual action by $G\gamma$ and $G\beta$ for optimal activation of GIRK channels in a channel subunit-specific manner

Galit Tabak¹, Tal Keren-Raifman¹, Uri Kahanovitch^{1,2} & Nathan Dascal¹

The tetrameric G protein-gated K^+ channels (GIRKs) mediate inhibitory effects of neurotransmitters that activate $G_{i/o}$ -coupled receptors. GIRKs are activated by binding of the $G\beta\gamma$ dimer, via contacts with $G\beta$. $G\gamma$ underlies membrane targeting of $G\beta\gamma$, but has not been implicated in channel gating. We observed that, in *Xenopus* oocytes, expression of $G\gamma$ alone activated homotetrameric GIRK1* and heterotetrameric GIRK1/3 channels, without affecting the surface expression of GIRK or $G\beta$. $G\gamma$ and $G\beta$ acted interdependently: the effect of $G\gamma$ required the presence of ambient $G\beta$ and was enhanced by low doses of coexpressed $G\beta$, whereas excess of either $G\beta$ or $G\gamma$ imparted suboptimal activation, possibly by sequestering the other subunit “away” from the channel. The unique distal C-terminus of GIRK1, G1-dCT, was important but insufficient for $G\gamma$ action. Notably, GIRK2 and GIRK1/2 were not activated by $G\gamma$. Our results suggest that $G\gamma$ regulates GIRK1* and GIRK1/3 channel’s gating, aiding $G\beta$ to trigger the channel’s opening. We hypothesize that $G\gamma$ helps to relax the inhibitory effect of a gating element (“lock”) encompassed, in part, by the G1-dCT; GIRK2 acts to occlude the effect of $G\gamma$, either by setting in motion the same mechanism as $G\gamma$, or by triggering an opposing gating effect.

G protein-gated inwardly rectifying K^+ channels (GIRK or Kir3) are a subfamily of tetrameric inwardly rectifying K^+ channels, with 4 genes encoding 4 GIRK subunits (GIRK1–4) in mammals^{1–3}. GIRKs mediate inhibitory actions of neurotransmitters that activate G protein-coupled receptors (GPCRs). GIRKs regulate neuronal excitability and are associated with a large number of neurological disorders and alcohol and drug addiction^{4–6}. GIRK1, GIRK2 and GIRK3 are widely expressed in the brain, showing overlapping but distinct distribution patterns in brain structures and within neurons^{4,7–9}. While GIRK1/2 is considered as most abundant brain channel, GIRK1/3 is also ubiquitous, and GIRK2 homotetramers abound in the substantia nigra^{10–14}. GIRK1 and GIRK3 cannot form homotetramers, but a pore mutation in GIRK1, F137S, allows its expression as a homotetramer, denoted as GIRK1*, which is instrumental for structure-function studies^{15–18}.

In response to neurotransmitters, following the GPCR-catalyzed separation of $G\beta\gamma$ from $G\alpha_{i/o}$, GIRKs are activated by direct binding of up to four $G\beta\gamma$ subunits^{19–28}. In addition to this GPCR-evoked activity (I_{evoked}), GIRKs also show basal activity (I_{basal}) that varies considerably between channels of different subunit combinations (reviewed in ref.²⁹). The complex, subunit-dependent interrelationships of GIRKs with G proteins are still incompletely understood.

GIRK1 contains a 121 amino acid-long distal C-terminus (G1-dCT) that endows GIRK1-containing channels with unique characteristics. This labile (and absent form crystal structures) protein segment does not strongly bind $G\beta\gamma$ but it imparts high functional activity upon GIRK1-containing channels^{30,31} and high-affinity binding (“anchoring”) of $G\beta\gamma$ to the full cytosolic domain of GIRK1^{18,32–34}. This is manifested in the recruitment of $G\beta\gamma$ – but not $G\alpha$ – to the vicinity of these channels and high I_{basal} of GIRK1-containing channels^{18,34}. G1-dCT may also carry out an additional function: it appears to contain an inhibitory element (“lock”) that reduces the extent of activation by $G\beta\gamma$ ^{18,34–36}.

Mutagenesis, structural and NMR studies indicate a major role for $G\beta$ in $G\beta\gamma$ interaction with, and activation of GIRKs^{26,27,37–40}. The $G\gamma$ is thought to be primarily responsible for membrane targeting and attachment of the

¹Department of Physiology and Pharmacology and Sagol School of Neuroscience, Sackler School of Medicine, Tel Aviv University, Tel Aviv, 69978, Israel. ²Present address: Virginia Tech School of Neuroscience, Blacksburg, VA, 24061, USA. Correspondence and requests for materials should be addressed to N.D. (email: dascaln@taux.tau.ac.il)

G $\beta\gamma$ dimer, through C-terminal prenylation of G γ ^{41–44}. G $\beta\gamma$ containing a non-prenylated mutant of G γ does not activate GIRKs, presumably because of deficient PM targeting^{45,46}. It is not known if G γ plays any role in GIRK gating, besides membrane targeting. A role for G γ in interactions and functional effects of G $\beta\gamma$ on several effectors has been proposed, among them adenylyl cyclase (AC) and phospholipase C β (PLC β)^{47–52}. A recent study has localized two key regions in the N-terminus of G γ subunit that may contribute to high-affinity binding of G $\beta_1\gamma_2$ to a ternary SNARE complex⁵³, suggesting that G γ may contribute to interaction with effectors through mechanisms besides prenylation. Kawano *et al.*⁵⁴ observed that C terminal mutants of G β , which do not bind G γ , are still able to associate with GIRK1 and GIRK2 in a co-immunoprecipitation assay, but cannot activate the GIRK1/2 channel. The authors proposed that G γ plays a more important role in GIRK gating besides aiding in membrane insertion of the G $\beta\gamma$ dimer⁵⁴; however, since G β cannot properly fold and reach the membrane without G γ (see Discussion), the interpretation of these results is not unequivocal.

Here we report that expression of G γ alone can activate GIRK channels in *Xenopus* oocytes. The activation is subunit-specific: GIRK1* and GIRK1/3 are activated, GIRK2 and GIRK1/2 are not. Unlike the expressed G $\beta\gamma$, which enhances I_{basal} but diminishes the agonist-evoked current, I_{evoked} , G γ increases I_{basal} but does not reduce, and under certain conditions even increases, I_{evoked} . Activation by G γ requires the presence of endogenous (ambient) G $\beta\gamma$ and shows a complex stoichiometric relationship with coexpressed G β , suggesting that G γ acts as a “helper” for G $\beta\gamma$ in opening the channel, possibly by removing an inhibitory constraint imposed by the “lock” present in the GIRK1 subunit.

Results

G γ enhances GIRK1* basal and evoked currents. In preliminary experiments, we serendipitously discovered that heterologous expression of G γ_2 , without G β , activated the GIRK1* channel. To define the role of G γ in GIRK1* regulation, we used two-electrode voltage clamp with standard protocols¹⁸ to measure whole-cell GIRK currents in *Xenopus* oocytes (Fig. 1A). At a holding potential of -80 mV, shift from the low-K⁺ ND96 solution (2 mM K⁺) to a high-K⁺ (24 or 96 mM K⁺) solution induced an inward current. This current is due mostly to the basal activity of the expressed GIRK channels; the endogenous K⁺ currents in *Xenopus* oocytes are very small under these conditions^{55,56}. Then the oocyte was perfused with HK solution containing 10 μ M acetylcholine (ACh) which produced an evoked current, I_{evoked} , due to the activation of coexpressed muscarinic m2 receptor, m2R. Full block of GIRK channels by 5 mM Ba²⁺ applied at the end of the protocol allowed calculation of net GIRK basal current, I_{basal} (Fig. 1A).

Throughout this study, we used the ubiquitous G β_1 and G γ_2 (G β and G γ in the following), which are the most abundant, PM-associated neuronal G β and G γ species⁵⁷. We first studied the effect of a range of doses of G γ RNA (“titration” of G γ expression). With GIRK1* expressed at 0.2 ng RNA/oocyte, G γ increased I_{basal} of GIRK1* up to 4-fold and I_{evoked} up to 3-fold (Fig. 1A–C). Interestingly, for both basal and evoked currents, the dose-response curve was bell-shaped (Fig. 1B,C). Maximal increase in I_{basal} of GIRK1* was usually obtained at relatively low doses of G γ RNA, 0.1–0.2 ng/oocyte (2.94 \pm 0.26 fold, $n = 41$ oocytes, $N = 3$ experiments). A higher dose of G γ_2 , 1–2 ng RNA per oocyte (typically used in experiments with GIRK), usually had a milder effect (1.79 \pm 0.1 fold increase in I_{basal} , $n = 106$, $N = 11$; see also summary in Fig. 2B).

G $\beta\gamma$ is a dimer in which the partner proteins enhance each other’s stability in the cell^{58,59}; however, there is evidence for stable expression of G γ derivatives, such as GFP-G γ heterologously expressed in *Dictyostelium discoideum*⁶⁰. We first addressed the possibility that heterologously expressed G γ activates GIRK1* by recruiting the endogenous G β to the PM and increasing the total surface G $\beta\gamma$ level. We examined whether expression of G γ affects the level of endogenous PM-attached G β using a method uniquely applicable to *Xenopus* oocytes, in which plasma membranes, together with the surrounding extracellular matrix (vitelline membrane), are manually separated from the rest of the oocyte^{61,62}. Fig. 1D shows a Western blot of isolated PMs from oocytes injected with RNA of GIRK1* alone or together with 0.2 ng G γ RNA. Coexpression of G γ did not significantly change the amount of endogenous G β in the PM. On average, the PM level of G β was 70 \pm 19% of control when 0.2 ng G γ was coexpressed of (Fig. 1E, $n = 5$; $p = 0.17$). These results indicate that expression of G γ at doses that cause maximal activation of GIRK1* is not associated with a significant recruitment of endogenous G β (although we cannot rule out subtle changes in PM G β levels which may not be detected by Western blotting).

It has been previously shown for GIRK1/4, GIRK1/2 and GIRK1* that expression of G $\beta\gamma$ increases I_{basal} but suppresses I_{evoked} ^{16,18,21}. In contrast, G γ expressed alone significantly increased both I_{basal} and I_{evoked} of GIRK1*, with a maximal effect at 0.1–0.2 ng RNA/oocyte (Fig. 2). Figure 2B,C summarizes a large amount of similar experiments that demonstrated a significant increase in both I_{basal} and I_{evoked} of GIRK1 by G γ , with a maximal effect at 0.1–0.2 ng RNA/oocyte. G β expressed alone had no effect on I_{basal} but reproducibly decreased the evoked current. This is another indication that GIRK1* activation by G γ is not due to recruitment of G β by G γ .

G γ and various G γ -based constructs increase GIRK1* currents but not GIRK1* surface density.

Fluorescently (YFP or CFP)-labeled G γ constructs are often used instead of wild-type (WT) G γ , e.g. for imaging. We tested how such G γ -based protein constructs affect GIRK1* currents. We tested G γ , YFP-G γ , YFP_{A207K}-G γ (the A207K mutation prevents dimerization of YFP or CFP⁶³) and CFP_{A207K}-G γ . Expression of all G γ constructs caused a significant increase in GIRK1*’s I_{basal} and I_{evoked} (Fig. 3A,B). Effect on I_{basal} was quantified as fold increase in I_{basal} . CFP_{A207K} and YFP_{A207K}-tagged G γ increased I_{basal} similarly to WT G γ . Interestingly, the YFP-G γ lacking the A207K mutation caused the strongest activation of GIRK1*, ~ 7 fold (Fig. 3A). To address the possibility that dimerization of this YFP-fused construct somehow contributes to increased potency of G γ activation of GIRK1*, we generated a G γ concatemeric construct (G γ tandem) consisting of two G γ subunits joined head-to-tail. Coexpression of the G γ tandem strongly activated GIRK1*, similarly to YFP-G γ (Fig. 3A,C); the dose dependency on RNA dose was bell-shaped, like in the WT G γ (Fig. 3C). These results indicate that formation of dimers enhances the potency of G γ . Interestingly, I_{evoked} was similarly, mildly potentiated by all G γ constructs tested

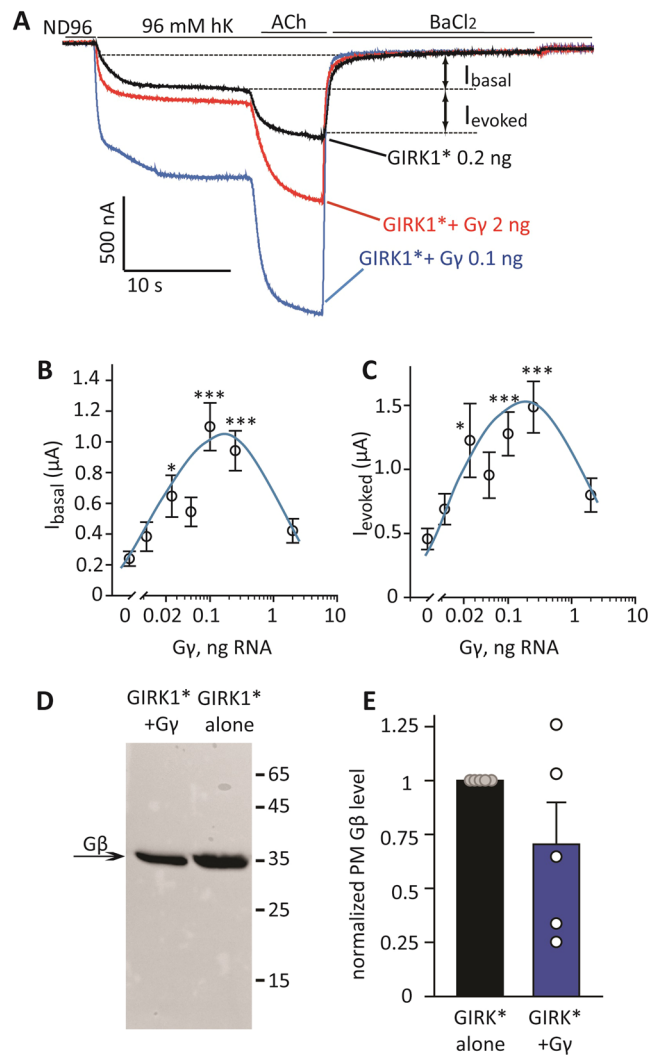


Figure 1. Expression of $G\gamma$ increases I_{basal} and I_{evoked} of GIRK1 without increasing the surface level of $G\beta$. **(A)** Representative records of GIRK currents showing that expression of $G\gamma$ (0.2 and 2 ng RNA/oocyte) increases I_{basal} and I_{evoked} of GIRK1*. GIRK1* was expressed at 0.2 ng RNA/oocyte together with m2R, 1 ng RNA/oocyte. Currents were first measured in a low- K^+ solution (ND96) which was switched to the high K^+ solution (hK, 96 or 24 mM K^+ , see Methods) resulting in an inward basal current, I_{hK} . Then the oocyte was perfused with hK solution containing 10 μM ACh, to produce I_{evoked} . At the end, 5 mM BaCl_2 was added to the solution to block GIRK currents and to reveal the residual non-GIRK current, I_{residual} . I_{basal} is defined as $I_{\text{hK}} - I_{\text{residual}}$, I_{evoked} as the net additional inward current evoked by ACh. Here I_{basal} and I_{evoked} are shown graphically for the control (GIRK1*) record. In $G\gamma$ - or $G\beta\gamma$ -expressing oocytes, the basal current is termed I_{I} or $I_{\text{I}\gamma}$, respectively, and defined as $I_{\text{hK}} - I_{\text{residual}}$. **(B,C)** Dose-dependence of the $G\gamma$ effect on I_{basal} and I_{evoked} . Increasing doses of $G\gamma$ RNA were injected, together with fixed amounts of RNAs of GIRK1* and m2R (same experiment as in A). Each point shown mean \pm SEM, $n = 9$ to 16 cells, $N = 1$ experiment. * $p < 0.05$; ** $p < 0.01$, *** $p < 0.001$. **(D)** Expression of $G\gamma$ does not alter the levels of $G\beta$ attached to the PM. The image shows Western blot of manually separated PMs (equal amounts of oocytes were used for each lane; here 25 oocytes/lane). The image was cropped from a larger one shown in Supplementary Fig. S1. Oocytes were injected with 0.2 ng of GIRK1* RNA, with or without 0.2 ng $G\gamma$ RNA. **(E)** Summary of 5 experiments ($N = 5$) of the kind shown in **(D)**. In each experiment, the $G\beta$ signal measured from the lane of $G\gamma$ -containing oocytes was normalized to $G\beta$ signal of control oocytes expressing GIRK1* only. Bars represent mean \pm SEM, circles show the results of individual experiments. There was no statistical difference in $G\beta$ level with or without coexpressed $G\gamma$, $p = 0.167$.

(Fig. 3B), underscoring the complexity of underlying mechanisms(s). In the following we routinely used YFP- $G\gamma$ and $G\gamma$ tandem, which produce a better channel activation than the WT $G\gamma$, and YFP tag allows measuring $G\gamma$ expression if needed. Key experiments have been repeated with WT $G\gamma$ to verify the authenticity of the observed phenomena.

Next, we set to test whether YFP- $G\gamma$ recruits GIRK1* to the PM (which could cause an increase in the whole-cell GIRK current). Oocytes were injected with two concentrations of RNA GIRK1*, 0.2 and 1 ng, with or without YFP- $G\gamma$ (2.5 ng RNA). Giant excised PM patches were prepared from the oocytes, stained with an

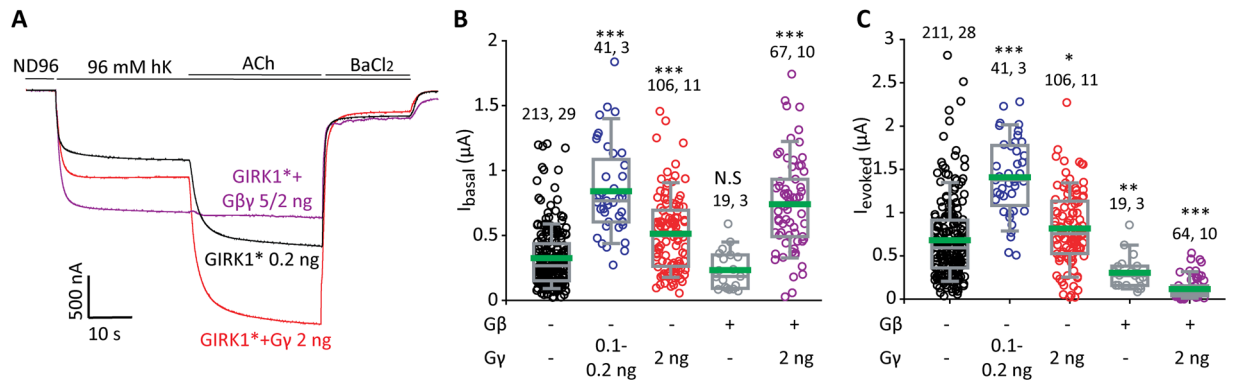


Figure 2. The effect of $G\gamma$ is different from the effect of coexpression of $G\beta\gamma$. **(A)** Representative currents in oocytes injected with the indicated concentrations of RNAs: $GIRK1^*$, $GIRK1^*$ with $G\gamma$, and $GIRK1^*$ with $G\beta\gamma$. $m2R$ was coexpressed in all cases. $G\gamma$ enhances both I_{basal} and I_{evoked} , whereas $G\beta\gamma$ enhances I_{basal} but abolishes I_{evoked} . **(B,C)** Summary of the effects of expression of $G\beta$, $G\gamma$ and $G\beta\gamma$ on I_{basal} and on I_{evoked} , respectively, of $GIRK1^*$. The RNA concentration of $GIRK1^*$ was 0.2 ng/oocyte, RNA concentrations of $G\beta$ and $G\gamma$ are indicated below the X axis. Data with 0.1 and 0.2 ng $G\gamma$ RNA were pulled because they produced very similar effects. The green line within the boxes shows the mean of data. Numbers at the top are n, N (number of cells, number of experiments). Statistical analysis: one-way ANOVA on ranks followed by Dunn's test. * $p < 0.05$, ** $p < 0.01$, *** $p < 0.001$, N.S = not significant, relative to $GIRK1^*$ alone.

antibody against $GIRK1$, and the expression was measured using a confocal microscope (Fig. 3D). Coexpression of YFP- $G\gamma$ did not increase the level of $GIRK1^*$ in the PM (Fig. 3D,E), whereas $GIRK1^*$ basal currents measured in the oocytes of the same batch were increased (Fig. 3F). We conclude that the increase of $GIRK1^*$ current, caused by coexpressed of $G\gamma$, is not due to an increase in the surface level of $GIRK1^*$ channels.

Interestingly, activation of $GIRK1^*$ (fold increase in I_{basal}) by both YFP- $G\gamma$ and YFP- $G\beta\gamma$ was milder for higher expression levels of $GIRK1^*$ (1–2 ng RNA) than for the lower expression level (0.2 ng RNA; Supplementary Fig. S2). The YFP- $G\gamma$ - induced increase in I_{evoked} was 1.48 ± 0.05 fold ($n = 152$; Figs 3B, S2) for low $GIRK1^*$ expression levels, and no increase in I_{evoked} was observed with high $GIRK1^*$ levels (0.95 ± 0.08 , $n = 34$; Figs 3F, S2). Poor activation by GPCR agonists and $G\beta\gamma$ at high levels of channel expression has been reported previously for $GIRK1^*$ ¹⁸ and $GIRK1/2$ ⁵⁴. In $GIRK1/2$, this phenomenon has been attributed to recruitment of free $G\beta\gamma$ by the channel, which results in increased basal activity and correspondingly reduced evoked responses^{34,62}. We assume that a similar process may take place in $GIRK1^*$ which also recruits $G\beta\gamma$ ³⁴, but have not further pursued this subject here.

Effect of $G\gamma$ on I_{basal} requires ambient $G\beta$. Since $G\beta$ is considered as the main $GIRK$ -interacting partner and activating moiety, we sought to investigate the possible involvement of $G\beta$ in $G\gamma$ -induced activation of $GIRK1^*$. To this end, we used phosducin, a $G\beta\gamma$ -binding protein which is widely used as a $G\beta\gamma$ “scavenger”^{65–67}. Phosducin interacts with $G\beta\gamma$ via contacts mainly in $G\beta$ subunit^{68,69}, therefore it is not expected to sequester any $G\gamma$ that is not associated with $G\beta$. We purified His-tagged phosducin (His-phosducin) and verified that it binds $G\beta\gamma$ (Supplementary Fig. S3A). We injected His-phosducin into the oocytes to a final concentration of $\sim 23 \mu M$ within the cell, at least 40–50 minutes before measuring currents (Fig. 4A). When $GIRK1^*$ was expressed alone, phosducin did not significantly reduce I_{basal} (Fig. 4D). We assume that, although $G\beta\gamma$ significantly contributes to I_{basal} in this channel¹⁸, the expected reduction in I_{basal} was obscured because of the relatively low I_{basal} observed in this experiment. In all other test groups, injection of His-phosducin into oocytes decreased $GIRK1^*$ current (Fig. 4B–D): by 74% for $GIRK1^*$ coexpressed with $G\beta\gamma$, by 79% for $GIRK1^*$ coexpressed with YFP- $G\gamma$, and by 63% for $GIRK1^*$ coexpressed with $G\beta + YFP-G\gamma$ (Fig. 4D). The inhibition of $G\gamma$ -YFP - induced $GIRK1^*$ activity suggests that the effect of $G\gamma$ depends on the presence of endogenous (ambient) $G\beta$.

An additional way of using phosducin was coexpression of myristoylated phosducin (myr-phosducin) by the injection of its RNA into the oocytes (Fig. 4E). The myristoylation tag at the N-terminus of myr-phosducin targets it to the membranes, including the PM⁶⁵. Expression of myr-phosducin significantly decreased I_{basal} of $GIRK1^*$ alone (Fig. 4H), as reported previously¹⁸. Myr-phosducin also inhibited $\sim 90\%$ of the $GIRK1^*$ current activated by coexpressed YFP- $G\gamma$ (Fig. 4G,H). Strikingly, when $GIRK1^*$ was activated by YFP- $G\gamma$ with coexpressed $G\beta$ (5 ng RNA), expression of myr-phosducin increased the current (Fig. 4F,H), or had no effect (Supplementary Fig. 3B). The possible reason for this seemingly paradoxical effect became clear only later, after titration of $G\beta$ concentrations (see Fig. 5 and the Discussion). We assumed that the expressed amount of phosducin is not sufficient to fully sequester all expressed $G\beta$ and therefore does not inhibit $GIRK1^*$ activation. In support, when we injected a lower dose of $G\beta$ (0.5 ng instead of 5 ng as in Fig. 4) together with YFP- $G\gamma$, activation of $GIRK1^*$ was very strong but phosducin almost completely inhibited it (Supplementary Fig. S3B). In summary, inhibition of YFP- $G\gamma$ - induced activation by coexpressed or added (as purified protein) phosducin, supports the notion that $G\gamma$ - induced activation of $GIRK1^*$ requires ambient $G\beta$.

Complex stoichiometric relationships between $G\gamma$ and $G\beta$. To better understand the mutual dependence of actions of $G\beta$ and $G\gamma$ on $GIRK1^*$, we titrated $G\beta$ RNA in the presence of a fixed concentration

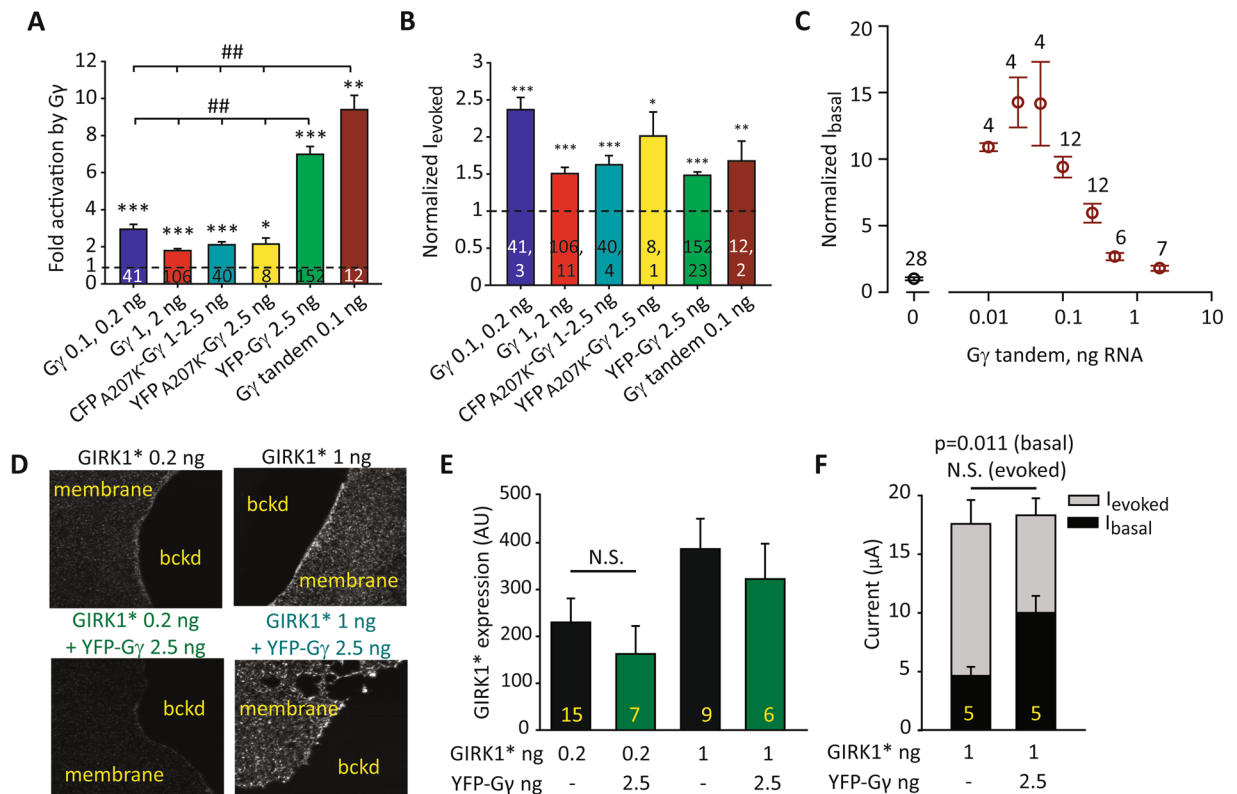


Figure 3. G γ and G γ -based constructs increase GIRK1* currents but not expression in PM. (A) Summary of GIRK1* activation by G γ , expressed as fold activation, for the different G γ constructs. Fold activation in all groups, including the control group, was calculated for each oocyte as the GIRK current in this oocyte, divided by the average current of the control group. For G γ and CFP_{A207K}-G γ , data obtained with 2 to 3 RNA doses that produced similar effects were pooled as indicated. Statistical analysis was performed using t-test for each G γ construct vs. control from the same experiments. * = < 0.05, ** < 0.01, *** < 0.001 in comparison to the control group, GIRK1* alone. In addition, the extent of activation was compared among all test groups using one-way ANOVA; ##, p < 0.01. (B) Summary of the effects of G γ constructs on I_{evoked}. Currents were normalized as follows: for each G γ construct, in each oocyte, including the oocytes of the control group (channel alone) the value of I_{evoked} was divided by the average I_{evoked} of the control group. Statistical analysis was performed using t-test, as in A. Numbers within columns show n, N (same for A and B). (C) Titrated expression of G γ tandem reveals a bell-shaped curve of dose-dependent activation of GIRK1* (0.2 ng RNA). Summary of N = 2 experiments. (D) Representative images of giant PM patches of oocytes expressing GIRK1* 0.2 ng or GIRK1* 1 ng alone (top) or with YFP-G γ 2.5 ng (bottom). N = 1 experiment. PM patches were stained with an antibody against GIRK1. Membranes are seen as brighter-colored areas, background is black. (E) Summary of GIRK1* expression at 0.2 and 1 ng with YFP-G γ 2.5 ng. Statistical analysis was performed by t-test. *p < 0.05, N.S., not statistically significant. A.U. - arbitrary units. (F) Summary of I_{basal} and I_{evoked} from the experiment in D and E, with oocytes injected with 1 ng GIRK1* RNA. The increase in I_{basal} in the presence of YFP-G γ was significant (p = 0.011), whereas I_{evoked} was not changed significantly (p = 0.101). Statistics: t-test on raw data.

of YFP-G γ RNA (2.5 ng/oocyte). As before, YFP-G γ increased both I_{basal} and I_{evoked} (Fig. 5A–C). Activation of GIRK1* by YFP-G γ was strongly affected by coexpression of G β in a complex manner. A low dose of G β (0.5 ng) enhanced the effect of YFP-G γ but higher doses of G β reversed this effect. G β γ still activated GIRK1*, but with higher levels of expressed G β the activation was even lower than with YFP-G γ alone (Fig. 5B). Strikingly, expression of even the lowest dose of G β , 0.5 ng RNA, suppressed I_{evoked} (Fig. 5C). Figure 5D,E summarize the effects of coexpression of YFP-G γ alone and with 5 ng G β from all experiments, showing that the reduction of YFP-G γ -induced activation of GIRK1* by a high dose of G β , and the suppression of I_{evoked}, were highly reproducible and significant. Similarly, low doses of G β potentiated activation of GIRK1* induced by WT G γ or YFP_{A207K}-G γ , and this effect was diminished when the dose of G β was increased (Supplementary Fig. S4). These results support the notion of mutual dependence of action of G γ and G β . It appears that overexpression of either G β (Fig. 5) or G γ (Fig. 1) is counterproductive for optimal channel activation, possibly through sequestration of one subunit by an excess of the other one (see Discussion).

G γ activates GIRK1/3 but not GIRK2 or GIRK1/2. We explored whether G γ affects neuronal GIRK channels of different subunit composition, starting with GIRK2. In contrast to GIRK1*, GIRK2 was not activated by G γ and showed a canonical activation by G β γ , with greater extent of activation with higher G β concentrations

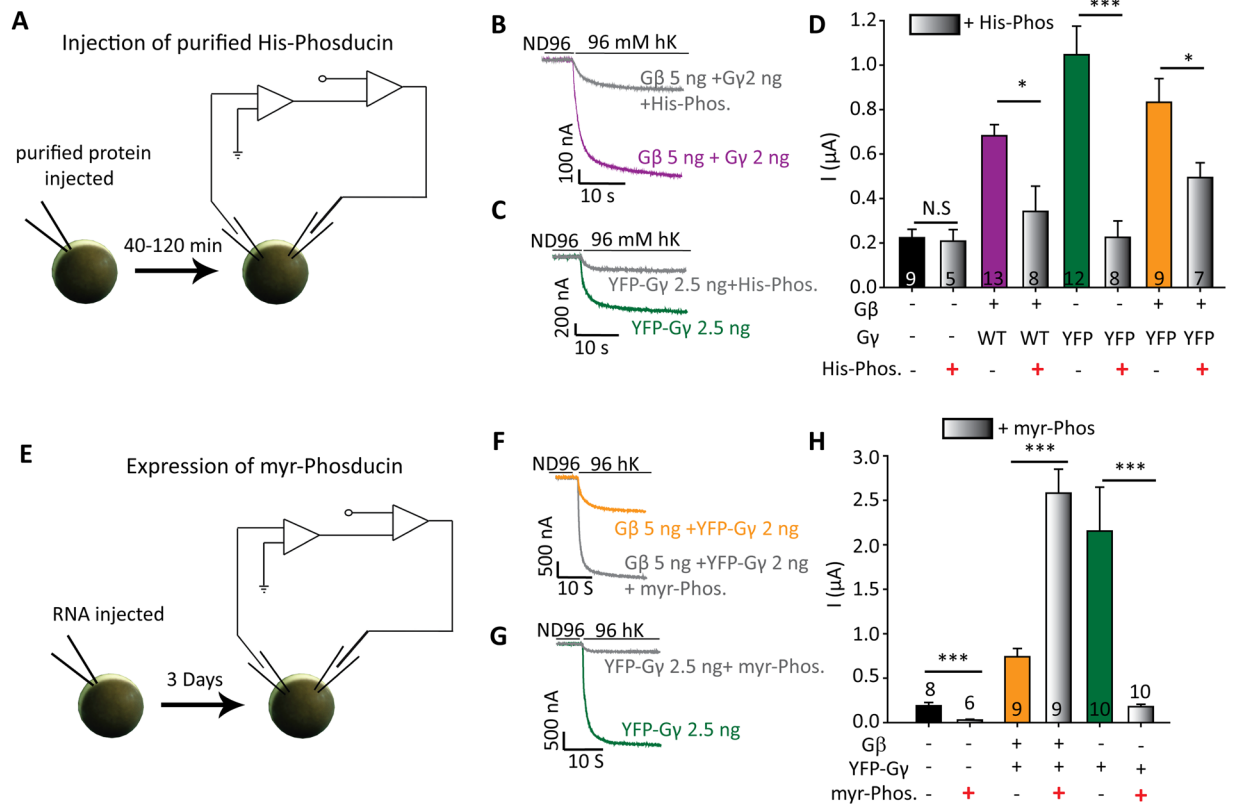


Figure 4. Activation of GIRK1* by G γ requires ambient G β . **(A–D)** Injection of purified His-phosducin (His-Phos) inhibits activation of GIRK1* by G γ . **(A)** Scheme of the experiment. At the day of the experiment, His-phosducin protein was injected into the oocytes to a final concentration of $\sim 23 \mu\text{M}$. After 40–50 min, currents were measured using the standard protocol. **(B,C)** Examples of GIRK1* currents. Oocytes were injected with GIRK1* 0.2 ng RNA/oocyte, G β 5 ng, YFP-G γ 2.5 ng or G γ 2 ng. Numbers of cells tested (n) are shown within bars; N = 1 experiment. **(D)** Summary of the experiment; His-phosducin significantly attenuates inward current measured in naïve oocytes in hK solution. Statistical analysis: t-test for each pair, with and without His-phosducin. * $p < 0.05$, ** $p < 0.01$, N.S - not statistically significant. **(E–H)** Coexpression of myr-phosducin abolishes activation of GIRK1* by YFP-G γ . **(E)** Scheme of the experiment. Myr-phosducin RNA (5 ng) was injected into the oocytes three days before the experiment, together with GIRK1* (0.2 ng RNA) and other indicated RNAs. **(F,G)** Examples of GIRK1* currents. **(H)** Summary of the results. Expression of myr-phosducin blocked the activation by YFP-G γ but, apparently paradoxically, enhanced activation caused by G β . Numbers of cells tested (n) are shown; N = 1 experiment. Statistical analysis was performed by using t-test for each pair, with and without myr-phosducin, *** $p < 0.001$.

(Fig. 6A,B). YFP-G γ also did not activate GIRK2 (Fig. 6C). Co-expression of G β with YFP-G γ increased $I_{\beta\gamma}$ as expected and to a similar extent as G β coexpressed with WT-G γ (Fig. 6C). The small decrease in I_{basal} of GIRK2 by YFP-G γ (Fig. 6C) may be due to changes in channel expression. These results indicate a specific role of GIRK1 subunit in mediating the effect of G γ .

Next, we tested the effects of G γ on GIRK1/2 and GIRK1/3, the most abundant neuronal GIRK channels. Fig. 7A,B shows a representative experiment in which GIRK1/3 was co-expressed with increasing doses of G γ RNA. G γ significantly increased I_{basal} up to a ~ 2 fold at 2 ng G γ RNA (Fig. 7A,B). Interestingly, unlike in GIRK1*, here we did not observe the bell-shaped dose-response relationship, but we have not tested higher doses of G γ . YFP-G γ and G γ tandem also significantly increased GIRK1/3 I_{basal} , about 5- and 2.5 fold, respectively (Fig. 7C,D). I_{evoked} was not significantly affected by WT-G γ ($104 \pm 9\%$ of control, $n = 12$, $N = 2$, not shown) but it was significantly increased by YFP-G γ ($153 \pm 11\%$, $p < 0.001$, $n = 46$, $N = 6$, not shown). In a separate experiment, we have monitored the effect of G γ tandem on surface expression of GIRK1/3 in giant excised PM patches (Supplementary Fig. S5). Titrated expression of RNA of the G γ tandem indicated that at concentration that produced maximal activation of GIRK1/3 (0.25 ng RNA, Supplementary Fig. S5C), the G γ tandem did not affect the level of GIRK1/3 in the PM. These experiments suggest that coexpression of G γ increases GIRK1/3 currents without affecting the channel's surface levels.

Unlike GIRK1* or GIRK1/3, the basal activity of GIRK1/2 was not affected by coexpression of G γ or YFP-G γ (Fig. 7E–G). I_{evoked} was also unaffected (not shown). Note that I_{basal} of GIRK1/2 was $> 4 \mu\text{A}$ (Fig. 7E,F) with a low dose of RNA, 0.05 ng RNA of each subunit. I_{basal} of GIRK2 was $0.36 \pm 0.05 \mu\text{A}$ ($n = 45$) with a 40-fold higher dose of RNA, 2 ng/oocyte (for review on I_{basal} differences in GIRK channels, see ref.²⁹). Therefore, $> 90\%$ of I_{basal} in this

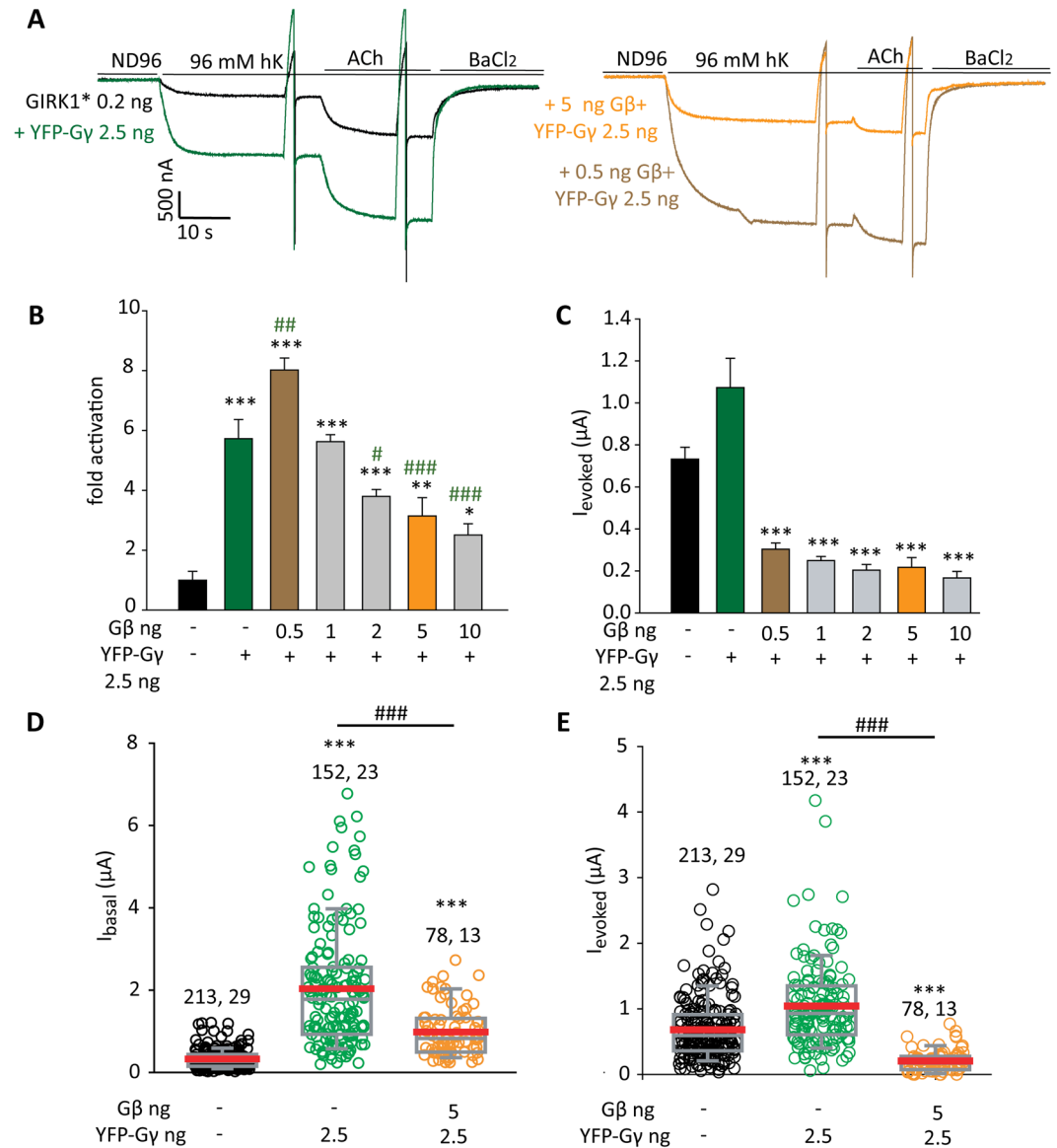


Figure 5. Complex stoichiometric relationships between $G\gamma$ and $G\beta$. (A–C) show one experiment in which RNA of $G\beta$ was varied whilst RNA of YFP- $G\gamma$ was constant, 2.5 ng RNA/oocyte. m2R (1 ng RNA) was coexpressed in all cases. (A) Representative current records in oocytes expressing GIRK1* (0.2 ng RNA) alone or with YFP- $G\gamma$, without or with $G\beta$ (0.5 or 5 ng RNA). Note that the basal current was larger when YFP- $G\gamma$ was coexpressed with 0.5 ng $G\beta$ than with 5 ng $G\beta$ RNA. The sharp deflections in traces are currents elicited by voltage ramps used to obtain current-voltage curves, which are not shown. (B) Summary of fold activation of GIRK1* (0.2 ng RNA) by $G\beta\gamma$ or $G\gamma$. $n = 7$ to 9 oocytes in each group, $N = 1$ experiment. Statistical analysis: asterisks * show difference from channel alone, pound signs # show difference from GIRK1 + YFP- $G\gamma$ (without $G\beta$). Compared to YFP- $G\gamma$ alone, coexpression of 0.5 ng $G\beta$ significantly increased I_{basal} ($p = 0.003$) but coexpression of 5 ng $G\beta$ reduced it ($p < 0.001$). One-way ANOVA (normal distribution) followed by Dunnett's test. (C) Summary of I_{evoked} . Expression of $G\gamma$ alone significantly elevated I_{evoked} ($p < 0.001$ by t-test). Comparison of groups expressing $G\beta$ and $G\gamma$ vs. GIRK1* + YFP- $G\gamma$ (green bar) was done using one-way ANOVA followed by Dunnett's test. *** $p < 0.001$. (D,E) show summary of the effects of YFP- $G\gamma$ vs. $G\beta$ + YFP- $G\gamma$ on I_{basal} and I_{evoked} of GIRK1* (0.2 ng RNA) from all experiments described in this report. Numbers at the top are n , N (number of cells, number of experiments). Statistical analysis: one-way ANOVA followed by Dunnett's test. *** $p < 0.001$ relative to GIRK1* alone. T-test was done to compare between GIRK1* co-expressed with YFP- $G\gamma$ vs. GIRK1* with $G\beta$ + YFP- $G\gamma$; ### $p < 0.001$.

case originated from GIRK1/2 heterotetramers rather than from any incidentally present GIRK2 homotetramers. We conclude that GIRK2 is not activated by $G\gamma$, and it also appears to prevent $G\gamma$ -induced activation of GIRK1 in a GIRK1/2 heterotetrameric context.

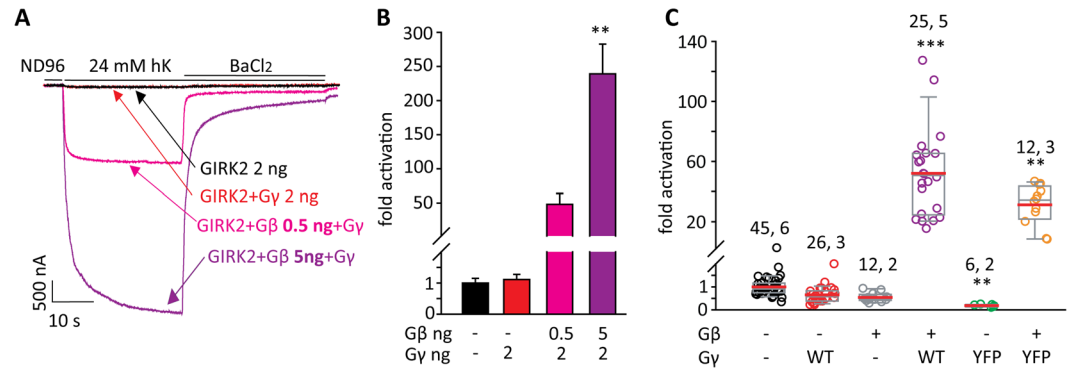


Figure 6. $G\gamma$ does not activate GIRK2. (A) Representative currents of GIRK2 (2 ng RNA) with two different concentrations of $G\beta$ RNA and a fixed concentration of $G\gamma$ RNA, 2 ng/oocyte. (B) Summary the representative experiment shown in A, showing fold activation by $G\gamma$ or $G\beta\gamma$ in each group. One-way ANOVA followed by Dunn's test. *, $p < 0.05$ relative to GIRK2 alone. $n = 5-6$ cells in each group; $N = 1$. (C) Summary of effects of $G\beta$, $G\beta\gamma$, $G\gamma$ and YFP- $G\gamma$ from this series of experiments. RNA doses, in ng/oocyte, were: GIRK2, 2; $G\gamma$, 1 or 2; $G\beta$, 5; YFP- $G\gamma$, 2.5. Numbers above data sets are n, N (number of cells, number of experiments). Statistical analysis: one-way ANOVA followed by Dunn's test. ** $p < 0.01$, *** $p < 0.001$ relative to GIRK2 alone.

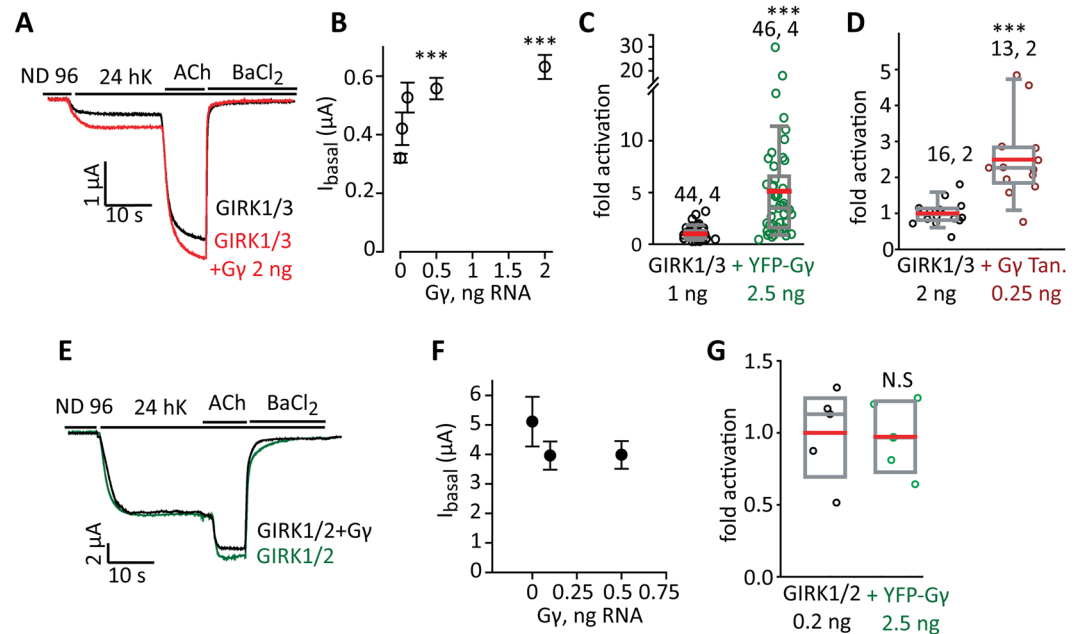


Figure 7. $G\gamma$ activates GIRK1/3 but not GIRK1/2. (A,B) Dose dependent activation of GIRK1/3 (1 ng RNA of each subunit) by $G\gamma$ (0.025-2 ng RNA). (A) Shows representative currents and (B) shows the full result of the experiment. $n = 14$ oocytes with each dose of $G\gamma$. Statistics: one-way ANOVA followed by Dunnett's test. *** $p < 0.001$ vs. GIRK1/3 alone. (C,D) Summary of effects of YFP- $G\gamma$ and $G\gamma$ tandem ($G\gamma$ Tan) on GIRK1/3. Numbers above data sets are n, N (number of cells, number of experiments). Statistics: t-test. (E,F) GIRK1/2 is not activated by $G\gamma$. Measurements were done in the same experiment as in A,B; the effect of $G\gamma$ on GIRK1/3 served as positive control. GIRK1/2 (0.05 ng RNA of each subunit) was coexpressed without or with two RNA doses of $G\gamma$, 0.1 or 0.5 ng. (E) Shows representative currents and (F) the full result of the experiment (5-9 cells in each group; $N = 1$). There was no significant difference between the groups. (G) YFP- $G\gamma$ does not activate GIRK1/2. There was no significant difference between the groups ($n = 5, N = 1$).

Distal C-terminus of GIRK1 (dCT) is important for $G\gamma$ -induced activation. We hypothesized that a structural difference between GIRK1* and GIRK2 may explain the divergent effects of $G\gamma$ on GIRK1* and GIRK2 in the homomeric context. One candidate structural element is the unique distal C-terminus of GIRK1, G1-dCT, which contributes to $G\beta\gamma$ anchoring and channel gating²⁹. Both GIRK2 and GIRK1*_{Δ121} (which is a deletion mutant of GIRK1* without the dCT) lack this element and cannot recruit $G\beta\gamma$. Accordingly, they have low basal activity and stronger relative activation by $G\beta\gamma$ compared to GIRK1* and GIRK1/2, suggesting that the $G\beta\gamma$ activation site in channel's core is intact^{18,34}.

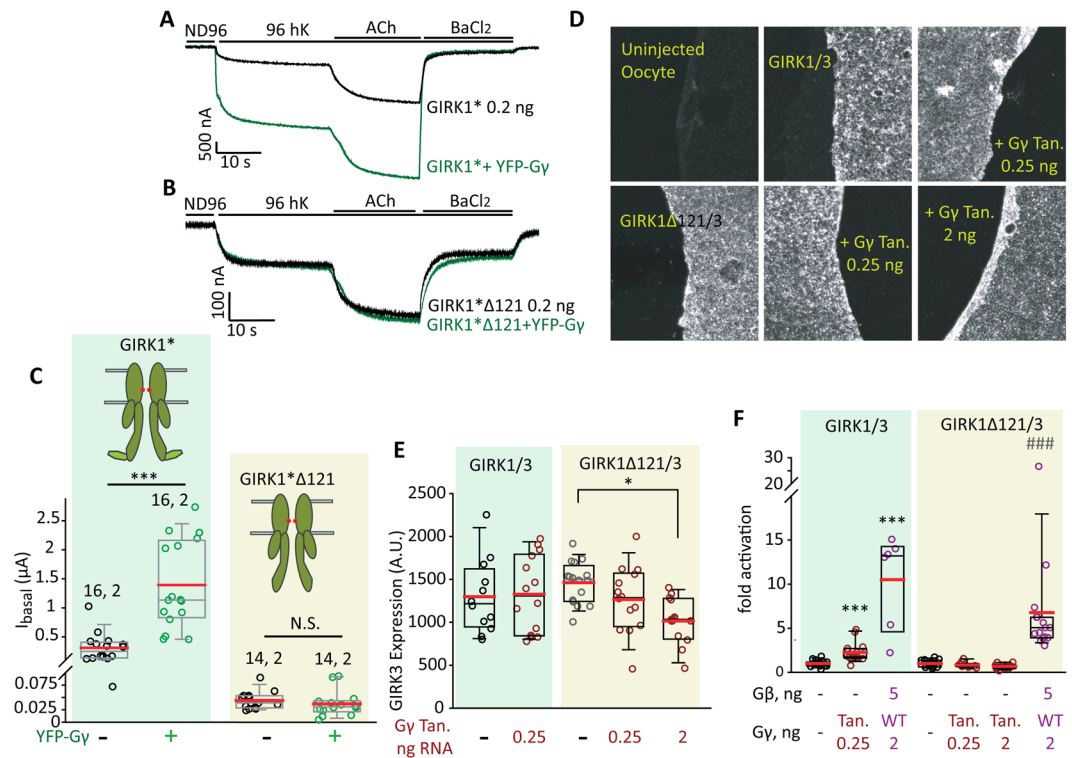


Figure 8. Distal C-terminus of GIRK1 is important for $G\gamma$ activation of GIRK1* and GIRK1/3. (A–C) Deletion of dCT abolishes the activating effect of YFP- $G\gamma$ (2.5 ng RNA) on GIRK1*. (A,B) show representative traces of GIRK1* (A) and GIRK1* $_{\Delta 121}$ (B) expressed alone or with YFP- $G\gamma$. m2R was expressed in all cases. (C) Summary of the experiment. Numbers above data sets are n, N. Statistics: t-test for each pair with and without YFP- $G\gamma$. *** $p < 0.001$, N.S., not statistically significant. (D–F) Expression of $G\gamma$ tandem ($G\gamma$ Tan) does not affect the expression of GIRK1/3 in the PM (D,E) and activates GIRK1/3 but not GIRK1 $_{\Delta 121}/3$ (GIRK1 $_{\Delta 121}/3$; F). Oocytes were stained with an antibody against GIRK3. Representative images of giant excised PM patches are shown in (D) and summary of measurements in (E) $G\gamma$ tandem did not affect the expression of GIRK1/3, but reduced the expression of GIRK1 $_{\Delta 121}/3$ when expressed at a high dose ($p < 0.05$ for 2 ng $G\gamma$ tandem). A.U., arbitrary units. $n = 12$ –16 membranes in each group, $N = 1$. (F) Summary of the effects of $G\gamma$ tandem and of $G\beta\gamma$ on I_{basal} . $n = 10$ –15 cells in each group, $N = 2$. $G\gamma$ tandem and $G\beta\gamma$ significantly increased I_{basal} of GIRK1/3 (*** $p \leq 0.001$ vs. GIRK1/3 alone). GIRK1 $_{\Delta 121}/3$ was not affected by $G\gamma$ tandem but was activated by $G\beta\gamma$ (### $p < 0.001$ vs. GIRK1 $_{\Delta 121}/3$ alone).

To assess the possible role of G1-dCT, we coexpressed YFP- $G\gamma$ with GIRK1* $_{\Delta 121}$. Figure 8A,B shows an exemplary experiment, Fig. 8C summarizes two experiments of this kind. YFP- $G\gamma$ had no effect on GIRK1* $_{\Delta 121}$ expressed at low density (0.2 ng RNA), whereas YFP- $G\gamma$ increased GIRK1* I_{basal} as expected (Fig. 8A–C). When GIRK1* $_{\Delta 121}$ was expressed at a higher level, 2 ng RNA, WT $G\gamma$ did not enhance I_{basal} , but YFP- $G\gamma$ appeared to produce a residual 2-fold activation of GIRK1* $_{\Delta 121}$ that did not reach statistical significance in one-way ANOVA test (Supplementary Fig. S6A). Notably, both WT $G\gamma$ and YFP- $G\gamma$ significantly reduced I_{evoked} of GIRK1* $_{\Delta 121}$, further underscoring the importance of G1-dCT for $G\gamma$ regulation of GIRK1* (Supplementary Fig. S6B). We also tested GIRK1 $_{\Delta 121}$ as a heterotetramer with GIRK3, GIRK1 $_{\Delta 121}/3$. This channel expressed well and its level in the PM was similar to that of GIRK1/3 containing the full-length GIRK1 subunit (Fig. 8D,E). Coexpression of $G\gamma$ tandem did not change the PM level of GIRK1/3; the PM level of GIRK1 $_{\Delta 121}/3$ was reduced by ~20% by the higher dose of $G\gamma$ tandem used, 2 ng RNA/oocyte (Fig. 8D,E). Unlike GIRK1/3, GIRK1 $_{\Delta 121}/3$ was not activated by coexpression of $G\gamma$ tandem (Fig. 8F). $G\beta\gamma$ strongly activated both GIRK1/3 and GIRK1 $_{\Delta 121}/3$ (Fig. 8F). Thus, removal of the G1-dCT significantly reduces the activating effect of $G\gamma$ on GIRK1* and GIRK1/3, suggesting a role for G1-dCT in this action of $G\gamma$.

We next wanted to test whether addition of G1-dCT to GIRK2 will render the channel sensitive to $G\gamma$. For this purpose, we used the chimera GIRK2HA/GIRK1dCT, which contains the G1-dCT (a.a. 371–501) fused to dCT-less GIRK2 (a.a. 1–381), as well as an extracellular HA tag (see cartoon in Fig. 9B). We have previously shown that C-terminal fusion of G1-dCT confers upon GIRK2HA the ability to recruit $G\beta\gamma$ to the PM; accordingly, this chimera has a much greater I_{basal} than GIRK2HA^{18,34}. However, YFP- $G\gamma$ did not activate the GIRK2HA/G1-dCT channel. In the same experiment, YFP- $G\gamma$ increased GIRK1* I_{basal} as expected (Fig. 9A,B). This result indicates that although G1-dCT is necessary for $G\gamma$ effect, it is not sufficient and possibly requires additional structural elements of the channel.

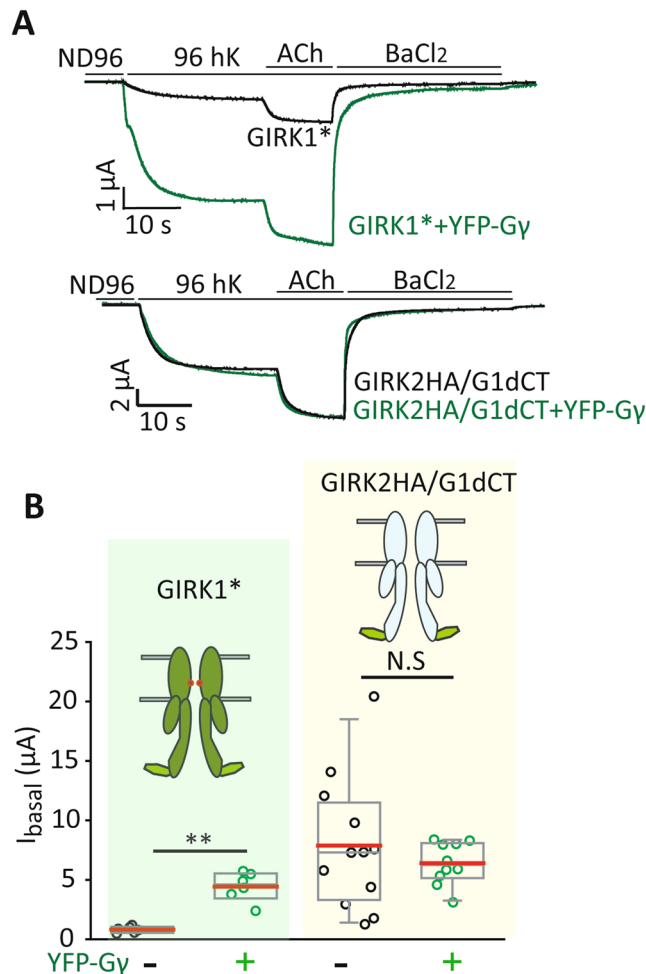


Figure 9. Addition of G1-dCT to GIRK2 does not confer G γ sensitivity. **(A)** Representative traces of GIRK1* (top) or GIRK2HA/G1-dCT (bottom), expressed alone (0.2 ng RNA) or with YFP-G γ (2.5 ng RNA). **(B)** Summary of the effect of YFP-G γ on I_{basal} . YFP-G γ activates GIRK1* but not GIRK2HA/G1-dCT. GIRK1*: n = 6, chimera alone: n = 12, chimera with YFP-G γ : n = 10, N = 1. **, p < 0.01, N.S. - not statistically significant (t-test for each construct with and without YFP-G γ).

Discussion

In performing its cellular functions, G $\beta\gamma$ acts as an obligatory, stable dimer, dissociated only by denaturation^{43,70}. G β and G γ are synthesized separately^{59,71}; dimerization greatly increases the stability of each subunit^{72–74}. Folding of G β requires the chaperone CCT complex, from which G β is released by the co-chaperone PhLP1^{59,71}. Mature G $\beta\gamma$ dimer is formed only after the binding of G γ ⁷⁵. Lipid modification (prenylation) of G γ is not required for association with G β , but is crucial for PM targeting of G $\beta\gamma$ and for activation of GIRKs^{45,46}. In accord with these cellular mechanisms, we found that heterologous expression of G β alone did not activate GIRK1* or GIRK2 channels (Figs 2, 6, S6).

Unlike G β , G γ can fold separately and is produced in cells in the absence of G β ^{71,76}, especially when fused to GFP, though still less than with G β ⁶⁰. We found that overexpression of G γ or G γ tagged with CFP or YFP enhances the activity of homomeric GIRK1* and heterotetrameric GIRK1/3 channels. Interestingly, the strongest activation was achieved by YFP-G γ without the A207K mutation, where YFP is prone to dimer formation⁶³. G γ tandem (concatemer) consisting of two fused G γ subunits activated GIRK1* and GIRK1/3 similarly to YFP-G γ (Figs 3, 7, 8), excluding a role for the xFP moiety in channel activation. No natural G γ dimer formation has been reported; but we hypothesize that artificial dimerization can protect against degradation and increase G γ 's stability. Alternatively, dimerization could be related to some steric aspect of the mechanism of action of G γ .

To address the action of G γ , we first considered the possibility that expression of G γ facilitates synthesis or trafficking to PM of GIRK1, which could account for the observed increase in I_{basal} and I_{evoked} . However, direct immunocytochemical measurements in giant excised PM patches consistently showed no change in the amount of GIRK1* and GIRK1/3 channel protein in the PM (Figs 3, 8, S5).

We then hypothesized that the expressed G γ may “recruit” G β to the PM. Absence of GIRK activation by expression of G β alone suggested that there was no free ambient (endogenous) G γ to form functional dimers with the expressed G β . It was plausible, however, that expression of exogenous G γ could enhance the release of

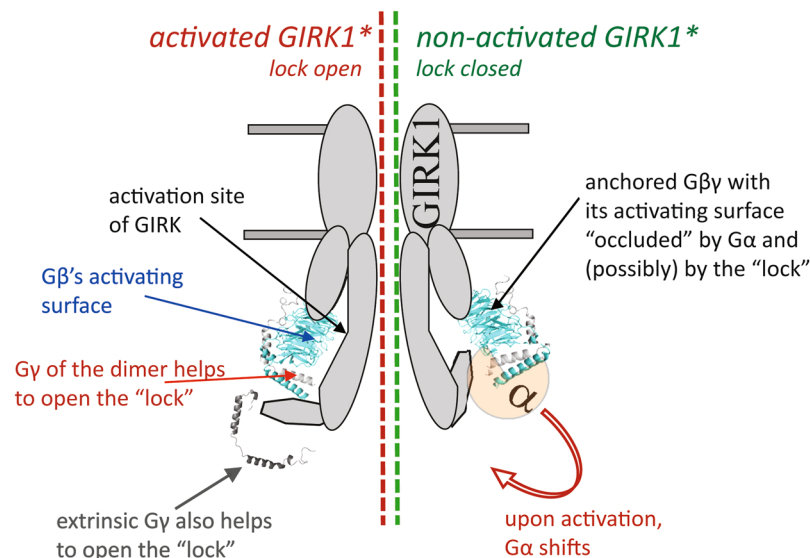


Figure 10. A hypothetical scheme of regulation of a GIRK channel containing the GIRK1 subunit by $G\gamma$. In GIRK1-containing channels, $G\beta\gamma$ or the $G\alpha\beta\gamma$ heterotrimer (shown in the figure) may be anchored to GIRK. In the resting state, the interaction surface of $G\beta$ is occluded by $G\alpha$ and cannot contact the activation site of GIRK. Lock element (encompassing the G1-dCT and other unknown parts of the channel) is closed, reducing channel activity. Upon activation by agonist, the GPCR (not shown) activates the G protein causing dissociation of $G\alpha$ from $G\beta\gamma$, exposing the GIRK-interacting surface of $G\beta$. $G\beta\gamma$ may now bind to the activation site. We propose that, at the same time, $G\gamma$ interacts with a channel's element and helps to release the inhibitory effect of the "lock". Exogenous $G\gamma$ may mimic this action without activating the channel by itself, but only if $G\beta\gamma$ is present.

ambient (endogenous) $G\beta$ trapped in the CCT⁷⁵, and in this way elevate the total $G\beta\gamma$ in the PM. However, several lines of evidence argue against the $G\beta$ recruitment hypothesis. First, we directly measured the PM levels of endogenous $G\beta$ using Western blots of manually separated PMs. Expression of $G\gamma$ at doses that produced robust activation of GIRK1* did not significantly change PM levels of $G\beta$ (Fig. 1). Second, $G\gamma$ and its derivatives did not decrease or (for low GIRK1* expression levels) increased I_{evoked} of GIRK1*, whereas expression of $G\beta\gamma$ always decreased it (Figs 2, 5, S2). This is incompatible with recruitment: even a small addition of $G\beta$ (if it were recruited by $G\gamma$) on top of $G\gamma$ would reduce I_{evoked} in GIRK1* (see Fig. 5). Third, expression of $G\gamma$ or YFP- $G\gamma$ did not activate either GIRK2, which is highly sensitive to expressed $G\beta\gamma$ ¹⁸ (Fig. 6), or GIRK1* $_{\Delta 121}$ that retains the GIRK1 $G\beta\gamma$ -activation site and is strongly activated by $G\beta\gamma$ ³⁴, or GIRK1 $_{\Delta 121/3}$ (Fig. 8). The inability of $G\gamma$ to activate these channels strongly argues against the $G\beta$ -recruitment hypothesis. All evidence considered, we conclude that changes in PM levels of either GIRK or $G\beta\gamma$ cannot explain the activating effect of $G\gamma$. We therefore propose that $G\gamma$ regulates the gating of GIRK1* and GIRK1/3.

How can $G\gamma$ regulate GIRK gating? A key insight into the mechanism of $G\gamma$ action comes from the finding that $G\gamma$ action is blocked by phosducin (Fig. 4). Phosducin interacts with $G\beta$ but not with $G\gamma$ ^{68,69}, implicating $G\beta$ in the effect of $G\gamma$. Another indication of the involvement of $G\beta$ is the enhancement of $G\gamma$ effect by coexpression of low doses of $G\beta$ (Figs 5, S4). Therefore, we suggest that the presence of ambient $G\beta$ is essential for the activation of GIRK1* and GIRK1/3 by $G\gamma$. Since the presence of free $G\beta$ in cells is unlikely, we propose that the effect of $G\gamma$ requires the presence of ambient $G\beta\gamma$, which is dynamically associated with the GIRK1-containing channels²⁹.

Another key insight came from the lack of GIRK2 activation by $G\gamma$ (Fig. 6). It implied the possible involvement of G1-dCT, which is unique to GIRK1, in $G\gamma$ regulation of GIRK1* and GIRK1/3. In support, deletion of G1-dCT greatly reduced the $G\gamma$ -induced activation of GIRK1* and GIRK1/3 (Figs 7, 8, S6) and completely abolished the $G\gamma$ -induced increase in I_{evoked} , causing a decrease instead (Fig. S6). To further address the function of G1-dCT, we used the chimera G2HA/G1-dCT in which the short dCT of GIRK2 (~34 amino acids) is replaced by G1-dCT. Addition of G1-dCT endows this chimera with an enhanced $G\beta\gamma$ binding compared to GIRK2; it also recruits $G\beta\gamma$ to the PM³⁴. However, the G2HA/G1-dCT channel was not affected by $G\gamma$ (Fig. 9), suggesting that G1-dCT alone is not sufficient to confer $G\gamma$ activation to GIRK2. Core elements in GIRK1 may also be involved; indeed, cross-talk between gating effects of G1-dCT and core of GIRK1 has been proposed³¹. Furthermore, since the G2HA/G1-dCT channel recruits $G\beta\gamma$, we posit that $G\gamma$ activation is not related to recruitment of $G\beta\gamma$. We hypothesize that it may be related to the second function of the G1-dCT, which is an inhibitory one, as explained below.

In light of these considerations, we propose a model (Fig. 10) in which $G\gamma$ aids $G\beta$ to drive the opening of GIRK1* and GIRK1/3 by acting on a gating element within the channel, rather than by participating in binding to the activation site. We envision that this function is normally carried out by $G\gamma$ from within the $G\beta\gamma$ dimer, e.g. when $G\beta\gamma$ is released from the $G\alpha\beta\gamma$ heterotrimer following GPCR-catalyzed GDP-GTP exchange (Fig. 10, "activated GIRK1*"). We propose that the coexpressed, properly prenylated $G\gamma$ can reach the vicinity of the channel and act on the same gating element, further helping $G\beta\gamma$ to shift the closed-open equilibrium in favor of the open

state. Since GIRK1/2 is not regulated by $G\gamma$, we propose that GIRK2 either counteracts or occludes the action of $G\gamma$; this will be discussed separately.

The nature of the gating element affected by $G\gamma$ is currently unclear. As a working hypothesis, we put forward the involvement of the hypothetical “lock” encompassed, in part, by the G1-dCT. A peptide corresponding to the last 20 amino acids of GIRK1 reduced the open probability (P_o) of $G\beta\gamma$ -activated GIRK1/5 and GIRK1/4 channels by a non-competitive mechanism, suggesting a gating effect rather than competition for $G\beta\gamma$ binding³⁶. Accordingly, the “lock”-deficient GIRK1* $_{\Delta 121}$ has a higher maximal $G\beta\gamma$ -induced P_o than GIRK1*³⁴. Thus, one of the possible scenarios of $G\gamma$ action could be the removal of the inhibitory effect of the “lock”, which would increase both I_{basal} and I_{evoked} by increasing the P_o of $G\beta\gamma$ -activated channels. We emphasize that other mechanisms in which $G\gamma$ allosterically regulates (enhances) the P_o will result in the same action. The proposed mechanism helps to explain, and is supported by, the findings obtained using the “expression pharmacology” approach^{62,77} (titration of protein expression in oocytes by injecting a range of RNA doses).

Finding #1: $G\gamma$ increases I_{basal} and I_{evoked} of GIRK1* and GIRK1/3, but expression of free $G\beta\gamma$ suppresses I_{evoked} (Figs 1–5). **Explanation:** $G\gamma$ acts by enhancing $G\beta\gamma$ -induced activation, irrespective of the source of $G\beta\gamma$ (a pre-associated “basal” $G\beta\gamma$ or $G\beta\gamma$ released from $G\alpha\beta\gamma$ through the activation of GPCR). Hence the increase both in I_{basal} and I_{evoked} . In contrast, coexpressed $G\beta\gamma$ suppresses I_{evoked} because it already maximally activates GIRK channels²¹, and also sequesters $G\alpha$ away from the GIRK-G protein complex, reducing activation by the GPCR¹⁸.

Finding #2: Expression of small amounts of $G\beta$ enhances the $G\gamma$ -induced activation better than higher amounts of $G\beta$ (Figs 5, S2). **Explanation:** GIRK1-containing channels are associated with excess of $G\beta$ over $G\alpha$ ²⁹, possibly already with 3–3.5 $G\beta\gamma$ molecules per channel⁶². A low dose of added $G\beta\gamma$ may suffice to reach the maximal stoichiometry of 4 $G\beta\gamma$ per one GIRK1* channel. Under these conditions, $G\gamma$ further increases P_o by further shifting closed-open equilibrium in favor of the open state. Expression of excess $G\beta$ and formation of more $G\beta\gamma$ dimers cannot cause further activation. However, it might decrease (sequester) free $G\gamma$ and reduce its concentration, counteracting the enhancing action of $G\gamma$.

Finding #3: Expression of high doses of $G\gamma$ produces a smaller activation of GIRK1* than an optimal, lower dose (Figs 1, 3). **Explanation:** similarly to the excess of $G\beta$, excess $G\gamma$ may be sequestering $G\beta$ “away from the channel”. However, more complex mechanisms cannot be excluded.

Finding #4: In the presence of coexpressed high dose of $G\beta\gamma$, expression of phosducin further increased I_{basal} (Fig. 4H). Rather counterintuitive, this finding is consistent with the proposed mechanistic framework. With 5 ng phosducin RNA, sequestration of $G\beta\gamma$ is probably incomplete^{56,65} and leaves a small amount of “extra” expressed $G\beta\gamma$. The latter, together with added coexpressed $G\gamma$, activates the channel to a high level, as explained above. In line with this, with low dose of $G\beta$ RNA (0.5 ng) phosducin effectively counteracted the action of $G\gamma$, supporting the role of $G\beta$ and underscoring the importance of stoichiometric considerations. Interestingly, the injected purified phosducin decreased channel activation in all conditions, suggesting a more complete $G\beta\gamma$ sequestration. Other possibilities, such as a long-term effect of coexpressed myr-phosducin on cellular levels of $G\beta\gamma$ or interactions within the signaling complex, cannot be ruled out.

In addition to mutual sequestration of $G\beta$, $G\gamma$ and phosducin, mechanisms that could contribute to the reduction in $G\gamma$ activation at high $G\gamma$ or $G\beta$ levels include the formation of inactive $G\beta\gamma$ oligomers or $G\gamma$ aggregates⁷⁴, or variation in stoichiometry of $G\alpha$ that may alter channel’s activity. In summary, we have found that stoichiometric relationships between expressed proteins crucially determine the observed regulations of GIRKs by $G\beta$ and $G\gamma$. Mutual sequestration or formation of protein oligomers of inadequate stoichiometry probably explain the complex, bell-shaped dose-response relationships of $G\gamma$ and $G\beta$ effects (Figs 1, 3, 5, S2). The new insights obtained here underscore the power of the “expression pharmacology” approach for studies of complex regulatory mechanisms in heterologous expression systems.

Importantly, GIRKs of different subunit composition showed diverse regulation by $G\gamma$. Only GIRK1/3 was regulated similarly to GIRK1*; GIRK2 and GIRK1/2 were not affected by $G\gamma$. These findings carry a potential physiological relevance because of the specific and diverse subunit composition of GIRKs in the brain. Furthermore, they may provide new insights as to the mechanism of $G\gamma$ action and, generally, of the regulation of GIRKs by G protein subunits. If, as we have proposed, $G\gamma$ allosterically regulates GIRK by acting on a gating element (such as the “lock” present in GIRK1), then GIRK2 may contain a structural element that exerts the same effect, whereas GIRK3 does not. In this way GIRK2 may occlude the effect of $G\gamma$. This would explain why GIRK1/3 is regulated by coexpression of $G\gamma$ whereas GIRK1/2 is not. Another possibility is that GIRK2 counteracts the effect of $G\gamma$ by acting on a different structural element within the GIRK1/2 heterotetramer.

Absence of activation of GIRK1/2 by coexpressed $G\gamma$ seems to be at odds with the previous finding that $G\gamma$ is essential for $G\beta$ to activate GIRK1/2⁵⁴. However, a more detailed examination of our and Kawano’s data reveals that there is no controversy. Kawano *et al.*⁵⁴ showed that mutated $G\beta$ that does not bind $G\gamma$ can still associate (at least it is co-immunoprecipitated) with GIRK subunits, but it cannot activate GIRK1/2. These results are supported by our data where $G\beta$ alone cannot activate any of the GIRK channels tested, and corroborate the notion that, without prenylation of $G\gamma$, $G\beta\gamma$ cannot reach the PM and cannot activate any GIRK channel^{45,46}. In comparison, our approach with expression of $G\gamma$ reveals unknown mechanistic aspects of $G\gamma$ action with physiologically relevant, functional $G\beta$ and $G\gamma$ proteins. Our results show that $G\gamma$ not only is essential for GIRK activation by the $G\beta\gamma$ dimer, but also actively supports the $G\beta\gamma$ -induced transition to open state.

Conclusions. We demonstrate that the $G\gamma$ subunit contributes to $G\beta\gamma$ -induced activation of GIRK channels in a GIRK subunit-specific manner. Expression of $G\gamma$ alone activated homotetrameric GIRK1* and heterotetrameric GIRK1/3 channels, but not GIRK2 or GIRK1/2. In GIRK1* and GIRK1/3, $G\gamma$ increases both I_{basal} and I_{evoked} , without affecting surface expression of the channels. Our results suggest that, besides its known role in targeting $G\beta\gamma$ to the plasma membrane, $G\gamma$ regulates the gating of GIRKs, in concert with $G\beta$. The unique distal

Construct	Species	Accession #	Comments
GIRK1*	Human	NM_002239	a pore mutation in GIRK1, F137S, allows its expression as a homotetramer
GIRK1	Rat	NM_031610.3	
GIRK1* _{Δ121}	Rat	NM_031610.3	Lacks the last 121 a.a., aka the G1-dCT
GIRK2	Mouse	NM_002240.4	
GIRK3	Rat	NM_053834.1	
GIRK2-dCTG1	Mouse (GIRK2), Rat (GIRK1)	NM_031610.3 (GIRK1) NM_002240.4 (GIRK2)	Chimera consist of GIRK2 (a.a. 1-381) and GIRK1 (a.a. 371-501).
Gβ ₁	Bovine	NM_175777.3	
YFP-Gγ ₂	Bovine (Gγ)	NM_174072.4	YFP without the A207K mutation
YFP _{A207K} -Gγ ₂	Bovine (Gγ)	NM_174072.4	YFP with the A207K mutation.
CFP _{A207K} -Gγ ₂	Bovine (Gγ)	NM_174072.4	CFP with the A207K mutation.
Gγ ₂ tandem	Bovine	NM_174072.4	Concatemer of two Gγ ₂ subunit with the linker Ser-Arg (encoded by XbaI sequence, TCTAGA). Gγ ₂ tandem was constructed using PCR followed by ligation.
Gγ ₂	Bovine	NM_174072.4	
m2R	Human	NM_001006630.1	
myr-phosducin	Bovine	NM_001166527.1	Phosducin with myristoylation tag
His-phosducin	Bovine	NM_001166527.1	Used for protein production

Table 1. List of cDNA constructs.

C-terminus of GIRK1, G1-dCT, is important but not sufficient for Gγ action. As a working hypothesis, we propose that Gγ regulates GIRK1* and GIRK1/3 channels by relaxing the inhibitory effect of the “lock” which is encompassed, in part, by the G1-dCT. We further hypothesize that, within the GIRK1/2 heterotetramer, GIRK2 acts to occlude the effect of Gγ, either by operating through the same mechanism as Gγ, or by triggering an opposing gating effect.

Methods

Ethical approval and animals. Experiments were approved by Tel Aviv University Institutional Animal Care and Use Committee (permits M-08-081 and M-13-002). All experiments were performed in accordance with relevant guidelines and regulations. *Xenopus laevis* female frogs were maintained and operated as described⁷⁸. Frogs were kept in dechlorinated water tanks at 20 ± 2 °C on 10 h light/14 h dark cycle, anesthetized in a 0.17% solution of procaine methanesulphonate (MS222), and portions of ovary were removed through a small incision in the abdomen. The incision was sutured, and the animal was held in a separate tank until it had fully recovered from the anesthesia and then returned to post-operational animals’ tank. The animals did not show any signs of post-operational distress and were allowed to recover for at least 3 months until the next surgery. Following the final collection of oocytes, after 4 surgeries at most, anesthetized frogs were killed by decapitation and double pithing.

DNA constructs, RNA and purified phosducin. cDNA constructs of YFP- or CFP- labeled and unlabeled GIRK subunits, Gβ₁, Gγ₂, m2R and myristoylated phosducin (myr-Phosducin) constructs were cloned into pGEM-HE, pGEM-HJ or pBS-MXT vectors, which are high expression oocyte vectors containing 5’ and 3’ untranslated sequences of *Xenopus* β-globin⁷⁹, as described^{65,80}. Constructs are described in Table 1. All PCR products were fully sequenced. Fluorescent xFP proteins (CFP_{A207K} and YFP_{A207K}) usually contained the A207K mutation that prevents their dimerization⁶³; however, when indicated, YFP was also used without the A207K mutation. Point mutations were introduced using PCR with the Pwo Master polymerase (Roche) according to manufacturer’s instructions, with primers containing the desired mutation. Afterwards, DpnI (New England Biolabs, R0176) was added to the reaction in order to degrade the template. The cDNA constructs were fully sequenced.

RNA was transcribed *in vitro* essentially as described⁷⁸ but precipitated overnight at −20 °C with 4 M LiCl instead of the standard ethanol/salt precipitation. RNA was divided into 1–2 μl aliquots and stored at −80 °C. The amounts of RNA injected per oocyte were varied according to the experimental design and are indicated in the results or in figure legends.

To prevent the formation of GIRK1*/GIRK5 heterotetramers, we injected the antisense oligonucleotide 5’T*A*AAT*CCC*TTG*CCA*TGA*T*G*G*T-3’ (*denotes phosphorothioate bond) targeted against the oocyte’s endogenous GIRK5 subunit of *Xenopus* GIRK5⁸¹ when studying GIRK1*, GIRK1/3 or GIRK chimeras.

For His-phosducin protein production, the coding sequence of bovine phosducin cDNA (see Table 1) was subcloned into pETMII vector which adds an N-terminal His-tag. Protein was amplified in BL-21 *E. coli*. Protein purification was done with Ni-NTA column using the following buffer: 50 mM KH₂PO₄, 20 mM Tris-HCl, 100 mM NaCl, 5 mM β-mercaptoethanol, 250 mM Imidazole. The size of His-phosducin is ~29 kDa and its initial concentration was 13.5 mg/ml, or 465 μM. The injection volume per oocyte was 50 nl, therefore the final concentration of His-phosducin was ~23 μM in each oocyte (assuming oocyte volume of ~1 μl).

Electrophysiology. Oocyte defolliculation, incubation and RNA injection were performed as described previously⁷⁸. Oocytes were defolliculated with collagenase (Type 1 A, Sigma) in Ca-free ND96 solution (see below) and injected with 50 nl of RNA, and incubated for 2–4 days in NDE solution (ND96 solution supplemented with 2.5 mM pyruvate and 50 µg/ml gentamicin) at 20 °C prior to testing. The standard ND96 solution contained (in mM): 96 NaCl, 2 KCl, 1 MgCl₂, 1 CaCl₂, 5 HEPES, and was titrated with NaOH to pH of 7.6–7.8. CaCl₂ was omitted in Ca-free ND96.

Whole-cell GIRK currents in oocytes were measured using two-electrode voltage clamp (TEVC) with Geneclamp 500 (Molecular Devices, Sunnyvale, CA, USA), using agarose cushion electrodes⁸² filled with 3 M KCl, with resistances of 0.1–0.5 MΩ. GIRK currents were measured at a holding potential of –80 mV in either the standard low-[K⁺] ND96 solution, or in high [K⁺] solution (HK). We used HK with either 24 mM [K]_{out} (in mM: 24 KCl, 72 NaCl, 1 CaCl₂, 1 MgCl₂ and 5 HEPES) or 96 mM [K]_{out} (in mM: 96 KCl, 2 NaCl, 1 CaCl₂, 1 MgCl₂ and 5 HEPES). pH of all solutions was 7.4–7.6. Currents were measured as explained in Fig. 1A. Net basal GIRK currents were calculated by subtracting the residual Ba²⁺-insensitive current recorded in each cell at the end of the recording protocol, or, on rare occasions, by subtracting average current recorded in naïve oocytes of the same experiment. Data acquisition and analysis were performed using the pCLAMP 9 or pCLAMP 10 software (Molecular Devices, Sunnyvale, CA, USA).

Measurement of Gβγ in plasma membrane (PM) by Western blotting. Plasma membranes were separated from the rest of the oocyte (“cytosol”) as described^{61,83}. In brief, PM together with the vitelline membranes (extracellular collagen-like matrix) was removed manually with fine forceps after a 5–15 min incubation of the oocyte in a low osmolarity solution (5 mM NaCl, 5 mM HEPES, and protease inhibitors (Roche Complete Protease Inhibitors Cocktail, 1 tablet/50 ml), pH = 7.5). The remainder of the cell (“cytosol”) was processed separately, after removing of nuclei by centrifugation for 10 min at 700 × g at 4 °C. PMs (18–25 per lane) were solubilized in 35 µl running buffer (2% SDS, 10% glycerol, 5% β-mercaptoethanol, 0.05% Bromophenol Blue, 62.5 mM Tris-HCl, pH 6.8). Samples were electrophoresed on 12% polyacrylamide-SDS gel and transferred to nitrocellulose membranes for Western blotting with previously characterized⁶² antibody against Gβ at 1:500 or 1:1000 dilution (Santa Cruz Biotechnology, SC-378). Goat Anti-Rabbit IgG Antibody, (H + L) HRP conjugate secondary antibody at 1:40,000 dilution was applied (Merck Millipore, AP307P). The signals were visualized using the SuperSignal kit (Thermo, 15168) and images were obtained with the fluorescent imager Fusion FX7 (Vilber Lourmat, Germany) and quantitated using the ImageJ software (National Institutes of Health, USA). Oocytes of stage 6⁸⁴ were used. These large cells have a rather constant size (~1 mm in diameter); the total amount of protein in the PM is considered uniform, and in Western blots of oocyte’s protein number of loaded oocytes rather than µg protein is routinely reported, and no normalization of measured amount of Gβ to a housekeeping protein is considered necessary (e.g. refs^{61,62,83,85}). The same amount of cells was used for each lane on the gel (Fig. 1D, Supplementary Fig. S1).

Giant excised PM patches. Giant excised PM patches were prepared, stained with antibodies and imaged as described⁸⁶. Oocytes were mechanically devitellinized using fine forceps in a hypertonic solution (in mM: NaCl 150, KCl 150, MgCl₂ 4, HEPES 10, pH 7.6). The devitellinized oocytes were transferred onto a ThermanoxTM coverslip (Nunc, Roskilde, Denmark) immersed in a Ca²⁺-free ND96 solution, with their animal pole facing the coverslip, for 10–20 minutes. The oocytes were then suctioned using a Pasteur pipette, leaving a giant membrane patch attached to the coverslip, with the cytosolic face toward the medium. The coverslip was washed thoroughly with fresh ND96 solution and fixated using 4% formaldehyde for 30 minutes. Fixated giant PM patches were immunostained in 5% milk in phosphate buffer solution (PBS). Non-specific binding was blocked with Donkey IgG 1:200 (Jackson ImmunoResearch, West Grove, PA, USA). Anti-Kir3.1 (GIRK1) antibody (Alomone labs, APC-005) or Anti-Kir3.3 (GIRK3) antibody (Alomone labs, APC-038) were applied at 1:200 or 1:100 dilution respectively, for 45 minutes at 37 °C. Anti-rabbit IgG DyLight650-labeled secondary antibody 1:400 (Abcam, ab96886) was then applied for 30 minutes in 37 °C, washed with PBS, and mounted on a slide for visualization. Immunostained slides were kept in 4 °C for no more than a week.

Confocal imaging. Confocal imaging and analysis were performed as described^{34,80}, with a Zeiss 510 META confocal microscope, using a 20x objective. In whole oocytes, the image was focused on oocyte’s animal (dark) hemisphere, at the equator. Images were acquired using spectral (λ)-mode: CFP was excited with a 405 nm laser and emission was collected at 481–492 nm. YFP was excited with the 514 nm line of the argon laser and emission was collected at 535–546 nm. Fluorescent signals were averaged from 3 regions of interest (ROI) at the PM and 3 similar ROIs from the coverslip outside the oocyte’s image, using Zeiss LSM Image Browser. The average background signal was subtracted from the average PM signal in each oocyte, and then the average net signal from the membrane of uninjected (naïve) oocytes was subtracted as well.

Imaging of proteins in giant PM patches was performed using the confocal microscope in λ-mode. DyLight650 was excited using 633 nm laser and emission was collected at 663–673 nm. Images centered on edges of the membrane patches, so that background fluorescence from coverslip could be seen. Two ROIs were chosen: one comprising most of the membrane patch within the field of view, and another comprising background fluorescence, which was subtracted from the signal obtained from the patch. The signal from giant PM patches of naïve oocytes’ membranes, immunostained using the same protocol, was subtracted from all groups.

Statistical analysis and data presentation. Imaging data on protein expression, as well as GIRK currents data collected from several experiments, have been normalized as described previously⁸⁷. Fluorescence intensity or current in each oocyte was normalized to the average signal in the oocytes of the control group of the

same experiment. This procedure yields average normalized intensity or current, as well statistical variability (e.g. SEM), in all treatment groups as well as in the control group. Statistical analysis was always performed on raw data with SigmaPlot 11 or SigmaPlot 13 (Systat Software Inc., San Jose, CA, USA). Two-group comparisons were performed using t-test if the data passed the Shapiro-Wilk normality test and the equal variance test, otherwise we used the Mann-Whitney Rank Sum Test. Multiple group comparisons were done using one-way ANOVA (ANOVA on ranks was performed whenever the data did not distribute normally). Tukey's or Dunnett's tests were performed for normally distributed data and Dunn's test otherwise. The data in the graphs are presented as mean \pm SEM or as raw data with superimposed box plots indicating 25–75 percentiles (box borders), median, mean (usually red line), and for some sets of data also 5–95 percentiles (whiskers).

Data Availability Statement

The data that support the findings of this study are available from the corresponding author, N.D, upon reasonable request.

References

1. Dascal, N. Signalling via the G protein-activated K⁺ channels. *Cell Signal* **9**, 551–573 (1997).
2. Jan, L. Y. & Jan, Y. N. Voltage-gated and inwardly rectifying potassium channels. *J Physiol* **505**(Pt 2), 267–282 (1997).
3. Hibino, H. *et al.* Inwardly rectifying potassium channels: their structure, function, and physiological roles. *Physiol Rev* **90**, 291–366 (2010).
4. Luscher, C. & Slesinger, P. A. Emerging roles for G protein-gated inwardly rectifying potassium (GIRK) channels in health and disease. *Nat Rev Neurosci* **11**, 301–315 (2010).
5. Lujan, R. M. F., de Velasco, E., Aguado, C. & Wickman, K. New insights into the therapeutic potential of Girk channels. *Trends Neurosci* **37**, 20–29 (2014).
6. Rifkin, R. A., Moss, S. J. & Slesinger, P. A. G protein-gated potassium channels: A link to drug addiction. *Trends Pharmacol Sci* **38**, 378–392 (2017).
7. Lujan, R. & Aguado, C. Localization and targeting of GIRK channels in mammalian central neurons. *Int Rev Neurobiol* **123**, 161–200 (2015).
8. Fernandez-Alacid, L. *et al.* Subcellular compartment-specific molecular diversity of pre- and post-synaptic GABA-activated GIRK channels in Purkinje cells. *J Neurochem* **110**, 1363–1376 (2009).
9. Fernandez-Alacid, L., Watanabe, M., Molnar, E., Wickman, K. & Lujan, R. Developmental regulation of G protein-gated inwardly-rectifying K⁺ (GIRK/Kir3) channel subunits in the brain. *Eur J Neurosci* **34**, 1724–1736 (2011).
10. Karschin, C. *et al.* Distribution and localization of a G protein-coupled inwardly rectifying K⁺ channel in the rat. *FEBS Lett* **348**, 139–144 (1994).
11. Kobayashi, T. *et al.* Molecular cloning of a mouse G-protein-activated K⁺ channel (mGIRK1) and distinct distributions of 3 GIRK (GIRK1, 2 and 3) mRNAs in mouse brain. *Biochem Biophys Res Commun* **208**, 1166–1173 (1995).
12. Inanobe, A. *et al.* Characterization of G-protein-gated K⁺ channels composed of Kir3.2 subunits in dopaminergic neurons of the substantia nigra. *J Neurosci* **19**, 1006–1017 (1999).
13. Koyrakh, L. *et al.* Molecular and cellular diversity of neuronal G-protein-gated potassium channels. *J Neurosci* **25**, 11468–11478 (2005).
14. Aguado, C. *et al.* Cell type-specific subunit composition of G protein-gated potassium channels in the cerebellum. *J Neurochem* **105**, 497–511 (2008).
15. Chan, K. W., Sui, J. L., Vivaudou, M. & Logothetis, D. E. Control of channel activity through a unique amino acid residue of a G protein-gated inwardly rectifying K⁺ channel subunit. *Proc Natl Acad Sci USA* **93**, 14193–14198 (1996).
16. Vivaudou, M. *et al.* Probing the G-protein regulation of GIRK1 and GIRK4, the two subunits of the K_{ACh} channel, using functional homomeric mutants. *J Biol Chem* **272**, 31553–31560 (1997).
17. Rogalski, S. L. & Chavkin, C. Eicosanoids inhibit the G-protein-gated inwardly rectifying potassium channel (Kir3) at the Na⁺/PIP₂ gating site. *J Biol Chem* **276**, 14855–14860 (2001).
18. Rubinstein, M. *et al.* Divergent regulation of GIRK1 and GIRK2 subunits of the neuronal G protein gated K⁺ channel by G_o and G_{βγ}. *J Physiol* **587**, 3473–3491 (2009).
19. Logothetis, D. E., Kurachi, Y., Galper, J., Neer, E. J. & Clapham, D. E. The βγ subunits of GTP-binding proteins activate the muscarinic K⁺ channel in heart. *Nature* **325**, 321–326 (1987).
20. Ito, H. *et al.* On the mechanism of G protein βγ subunit activation of the muscarinic K⁺ channel in guinea pig atrial cell membrane. Comparison with the ATP-sensitive K⁺ channel. *J Gen Physiol* **99**, 961–983 (1992).
21. Reuveny, E. *et al.* Activation of the cloned muscarinic potassium channel by G protein βγ subunits. *Nature* **370**, 143–146 (1994).
22. Krapivinsky, G., Krapivinsky, L., Wickman, K. & Clapham, D. E. G_{βγ} binds directly to the G protein-gated K⁺ channel, I_{KACH}. *J Biol Chem* **270**, 29059–29062 (1995).
23. Leaney, J. L. & Tinker, A. The role of members of the pertussis toxin-sensitive family of G proteins in coupling receptors to the activation of the G protein-gated inwardly rectifying potassium channel. *Proc Natl Acad Sci USA* **97**, 5651–5656 (2000).
24. Yamada, M. *et al.* GK* and brain G_{βγ} activate muscarinic K⁺ channel through the same mechanism. *J Biol Chem* **268**, 24551–24554 (1993).
25. Ivanova-Nikolova, T. T. & Breitwieser, G. E. Effector contributions to G_{βγ}-mediated signaling as revealed by muscarinic potassium channel gating. *J Gen Physiol* **109**, 245–253 (1997).
26. Yokogawa, M., Osawa, M., Takeuchi, K., Mase, Y. & Shimada, I. NMR analyses of the G_{βγ} binding and conformational rearrangements of the cytoplasmic pore of G protein-activated inwardly rectifying potassium channel 1 (GIRK1). *J Biol Chem* **286**, 2215–2223 (2011).
27. Whorton, M. R. & MacKinnon, R. X-ray structure of the mammalian GIRK2-βγ G-protein complex. *Nature* **498**, 190–197 (2013).
28. Wang, W., Touhara, K. K., Weir, K., Bean, B. P. & MacKinnon, R. Cooperative regulation by G proteins and Na⁺ of neuronal GIRK2 K⁺ channels. *Elife* **5**, e15751 (2016).
29. Dascal, N. & Kahanovitch, U. The roles of G_{βγ} and G_o in gating and regulation of GIRK channels. *Int Rev Neurobiol* **123**, 27–85 (2015).
30. Chan, K. W., Sui, J. L., Vivaudou, M. & Logothetis, D. E. Specific regions of heteromeric subunits involved in enhancement of G protein-gated K⁺ channel activity. *J Biol Chem* **272**, 6548–6555 (1997).
31. Wydeven, N., Young, D., Mirkovic, K. & Wickman, K. Structural elements in the Girk1 subunit that potentiate G protein-gated potassium channel activity. *Proc Natl Acad Sci USA* **109**, 21492–21497 (2012).
32. Ivanina, T. *et al.* Mapping the G_{βγ}-binding sites in GIRK1 and GIRK2 subunits of the G protein-activated K⁺ channel. *J Biol Chem* **278**, 29174–29183 (2003).
33. Huang, C. L., Jan, Y. N. & Jan, L. Y. Binding of the G protein βγ subunit to multiple regions of G protein-gated inward-rectifying K⁺ channels. *FEBS Lett* **405**, 291–298 (1997).

34. Kahanovitch, U. *et al.* Recruitment of G $\beta\gamma$ controls the basal activity of G-protein coupled inwardly rectifying potassium (GIRK) channels: crucial role of distal C terminus of GIRK1. *J Physiol* **592**, 5373–5390 (2014).
35. Dascal, N. *et al.* Inhibition of function in *Xenopus* oocytes of the inwardly rectifying G-protein-activated atrial K channel (GIRK1) by overexpression of a membrane-attached form of the C-terminal tail. *Proc Natl Acad Sci USA* **92**, 6758–6762 (1995).
36. Luchian, T. *et al.* A C-terminal peptide of the GIRK1 subunit directly blocks the G protein-activated K⁺ channel (GIRK) expressed in *Xenopus* oocytes. *J Physiol* **505**(Pt 1), 13–22 (1997).
37. Ford, C. E. *et al.* Molecular basis for interactions of G protein $\beta\gamma$ subunits with effectors. *Science* **280**, 1271–1274 (1998).
38. Albsoul-Younes, A. M. *et al.* Interaction sites of the G protein β subunit with brain G protein-coupled inward rectifier K⁺ channel. *J Biol Chem* **276**, 12712–12717 (2001).
39. Mirshahi, T., Robillard, L., Zhang, H., Hebert, T. E. & Logothetis, D. E. G β residues that do not interact with G α underlie agonist-independent activity of K⁺ channels. *J Biol Chem* **277**, 7348–7355 (2002).
40. Mahajan, R. *et al.* A computational model predicts that G $\beta\gamma$ acts at a cleft between channel subunits to activate GIRK1 channels. *Sci Signal* **6**, ra69 (2013).
41. Wedegaertner, P. B., Wilson, P. T. & Bourne, H. R. Lipid modifications of trimeric G proteins. *J Biol Chem* **270**, 503–506 (1995).
42. Ross, E. M. Protein modification. Palmitoylation in G-protein signaling pathways. *Curr Biol* **5**, 107–109 (1995).
43. Clapham, D. E. & Neer, E. J. G protein $\beta\gamma$ subunits. *Annu Rev Pharmacol Toxicol* **37**, 167–203 (1997).
44. Saini, D. K., Chisari, M. & Gautam, N. Shuttling and translocation of heterotrimeric G proteins and Ras. *Trends Pharmacol Sci* **30**, 278–286 (2009).
45. Schreiber, W. *et al.* Inhibition of an inwardly rectifying K channel by G-protein α -subunits. *Nature* **380**, 624–627 (1996).
46. Nakajima, Y., Nakajima, S. & Kozasa, T. Activation of G protein-coupled inward rectifier K⁺ channels in brain neurons requires association of G protein $\beta\gamma$ subunits with cell membrane. *FEBS Lett* **390**, 217–220 (1996).
47. Iniguez-Lluhi, J. A., Simon, M. I., Robishaw, J. D. & Gilman, A. G. G protein $\beta\gamma$ subunits synthesized in Sf9 cells. Functional characterization and the significance of prenylation of γ . *J Biol Chem* **267**, 23409–23417 (1992).
48. Yasuda, H., Lindorfer, M. A., Woodfork, K. A., Fletcher, J. E. & Garrison, J. C. Role of the prenyl group on the G protein γ subunit in coupling trimeric G proteins to A1 adenosine receptors. *Journal of Biological Chemistry* **271**, 18588–18595 (1996).
49. Myung, C. S. & Garrison, J. C. Role of C-terminal domains of the G protein β subunit in the activation of effectors. *Proc Natl Acad Sci USA* **97**, 9311–9316 (2000).
50. Myung, C. S., Yasuda, H., Liu, W. W., Harden, T. K. & Garrison, J. C. Role of isoprenoid lipids on the heterotrimeric G protein γ subunit in determining effector activation. *J Biol Chem* **274**, 16595–16603 (1999).
51. Fogg, V. C. *et al.* Role of the γ subunit prenyl moiety in G protein $\beta\gamma$ complex interaction with phospholipase C β . *J Biol Chem* **276**, 41797–41802 (2001).
52. Akgoz, M., Azpiazu, I., Kalyanaraman, V. & Gautam, N. Role of the G protein γ subunit in $\beta\gamma$ complex modulation of phospholipase C β function. *J Biol Chem* **277**, 19573–19578 (2002).
53. Zurawski, Z. *et al.* G $\beta\gamma$ directly modulates vesicle fusion by competing with synaptotagmin for binding to neuronal SNARE proteins embedded in membranes. *J Biol Chem* **292**, 12165–12177 (2017).
54. Kawano, T. *et al.* Importance of the G protein γ subunit in activating G protein-coupled inward rectifier K⁺ channels. *FEBS Lett* **463**, 355–359 (1999).
55. Dascal, N. *et al.* Expression of an atrial G-protein-activated potassium channel in *Xenopus* oocytes. *Proc Natl Acad Sci USA* **90**, 6596–6600 (1993).
56. Rubinstein, M., Peleg, S., Berlin, S., Brass, D. & Dascal, N. G α_{13} primes the G protein-activated K⁺ channels for activation by coexpressed G $\beta\gamma$ in intact *Xenopus* oocytes. *J Physiol* **581**, 17–32 (2007).
57. Yim, Y. Y. *et al.* Quantitative multiple-reaction monitoring proteomic analysis of G β and G γ subunits in C57Bl6/J brain synaptosomes. *Biochemistry* **56**, 5405–5416 (2017).
58. Dingus, J. *et al.* G protein $\beta\gamma$ dimer formation: G β and G γ differentially determine efficiency of *in vitro* dimer formation. *Biochemistry* **44**, 11882–11890 (2005).
59. Willardson, B. M. & Tracy, C. M. Chaperone-mediated assembly of G protein complexes. *Subcell Biochem* **63**, 131–153 (2012).
60. Knol, J. C., Engel, R., Blaauw, M., Visser, A. J. & van Haastert, P. J. The phosducin-like protein PhLP1 is essential for G $\beta\gamma$ dimer formation in *Dictyostelium discoideum*. *Mol Cell Biol* **25**, 8393–8400 (2005).
61. Sadler, S. E. & Maller, J. L. Progesterone inhibits adenylate cyclase in *Xenopus* oocytes. Action on the guanine nucleotide regulatory protein. *J Biol Chem* **256**, 6368–6373 (1981).
62. Yakubovich, D. *et al.* A quantitative model of the GIRK1/2 channel reveals that its basal and evoked activities are controlled by unequal stoichiometry of G α and G $\beta\gamma$. *PLoS Comput Biol* **11**, e1004598 (2015).
63. Zacharias, D. A., Violin, J. D., Newton, A. C. & Tsien, R. Y. Partitioning of lipid-modified monomeric GFPs into membrane microdomains of live cells. *Science* **296**, 913–916 (2002).
64. Peleg, S., Varon, D., Ivanina, T., Dessauer, C. W. & Dascal, N. G α_i controls the gating of the G-protein-activated K⁺ channel, GIRK. *Neuron* **33**, 87–99 (2002).
65. Rishal, I., Porozov, Y., Yakubovich, D., Varon, D. & Dascal, N. G $\beta\gamma$ -dependent and G $\beta\gamma$ -independent basal activity of G protein-activated K⁺ channels. *J Biol Chem* **280**, 16685–16694 (2005).
66. Riven, I., Iwanir, S. & Reuveny, E. GIRK channel activation involves a local rearrangement of a preformed G protein channel complex. *Neuron* **51**, 561–573 (2006).
67. Kienitz, M. C., Mintert-Jancke, E., Hertel, F. & Pott, L. Differential effects of genetically-encoded G $\beta\gamma$ scavengers on receptor-activated and basal Kir3.1/Kir3.4 channel current in rat atrial myocytes. *Cell Signal* **26**, 1182–1192 (2014).
68. Gaudet, R., Bohm, A. & Sigler, P. B. Crystal structure at 2.4 Å resolution of the complex of transducin $\beta\gamma$ and its regulator, phosducin. *Cell* **87**, 577–588 (1996).
69. Loew, A., Ho, Y.-K., Blundell, T. & Bax, B. Phosducin induces a structural change in transducin $\beta\gamma$. *Structure* **6**, 1007–1019 (1998).
70. Preininger, A. M. & Hamm, H. E. G protein signaling: insights from new structures. *Sci STKE* **2004**, re3 (2004).
71. Dingus, J. & Hildebrandt, J. D. Synthesis and assembly of G protein $\beta\gamma$ dimers: comparison of *in vitro* and *in vivo* studies. *Subcell Biochem* **63**, 155–180 (2012).
72. Schmidt, C. J. & Neer, E. J. *In vitro* synthesis of G protein $\beta\gamma$ dimers. *J Biol Chem* **266**, 4538–4544 (1991).
73. Higgins, J. B. & Casey, P. J. *In vitro* processing of recombinant G protein γ subunits. Requirements for assembly of an active $\beta\gamma$ complex. *J Biol Chem* **269**, 9067–9073 (1994).
74. Mende, U., Schmidt, C. J., Yi, F., Spring, D. J. & Neer, E. J. The G protein γ subunit. Requirements for dimerization with β subunits. *J Biol Chem* **270**, 15892–15898 (1995).
75. Plimpton, R. L. *et al.* Structures of the G β -CCT and PhLP1-G β -CCT complexes reveal a mechanism for G-protein β -subunit folding and G $\beta\gamma$ dimer assembly. *Proc Natl Acad Sci USA* **112**, 2413–2418 (2015).
76. Lukov, G. L. *et al.* Mechanism of assembly of G protein $\beta\gamma$ subunits by protein kinase CK2-phosphorylated phosducin-like protein and the cytosolic chaperonin complex. *J Biol Chem* **281**, 22261–22274 (2006).
77. Vorobiov, D., Bera, A. K., Keren-Raifman, T., Barzilai, R. & Dascal, N. Coupling of the muscarinic m2 receptor to G protein-activated K⁺ channels via G α_z and a receptor-G α_z fusion protein. Fusion between the receptor and G α_z eliminates catalytic (collision) coupling. *J. Biol. Chem.* **275**, 4166–4170 (2000).

78. Dascal, N. & Lotan, I. In *Protocols in Molecular Neurobiology* (eds Longstaff, A. & Revest, P.) 205–225 (Humana Press, Totowa, NJ, 1992).
79. Liman, E. R., Tytgat, J. & Hess, P. Subunit stoichiometry of a mammalian K⁺ channel determined by construction of multimeric cDNAs. *Neuron* **9**, 861–871 (1992).
80. Berlin, S. *et al.* Two distinct aspects of coupling between G α_{i3} protein and G protein-activated K⁺ channel (GIRK) revealed by fluorescently labeled G α_{i3} protein subunits. *J Biol Chem* **286**, 33223–33235 (2011).
81. Hedin, K. E., Lim, N. F. & Clapham, D. E. Cloning of a *Xenopus laevis* inwardly rectifying K⁺ channel subunit that permits GIRK1 expression of I_{KACH} currents in oocytes. *Neuron* **16**, 423–429 (1996).
82. Schreibmayer, W., Lester, H. A. & Dascal, N. Voltage clamping of *Xenopus laevis* oocytes utilizing agarose-cushion electrodes. *Pflugers Archive - European Journal of Physiology* **426**, 453–458 (1994).
83. Ivanina, T. *et al.* Phosphorylation by protein kinase A of RCK1 K⁺ channels expressed in *Xenopus* oocytes. *Biochemistry* **33**, 8786–8792 (1994).
84. Dumont, J. N. Oogenesis in *Xenopus laevis* (Daudin). I. Stages of oocyte development in laboratory maintained animals. *J Morphol* **136**, 153–179 (1972).
85. Tian, J., Kim, S., Heilig, E. & Ruderman, J. V. Identification of XPR-1, a progesterone receptor required for *Xenopus* oocyte activation. *Proc Natl Acad Sci USA* **97**, 14358–14363 (2000).
86. Singer-Lahat, D., Dascal, N., Mittelman, L., Peleg, S. & Lotan, I. Imaging plasma membrane proteins in large membrane patches of *Xenopus* oocytes. *Pflugers Arch* **440**, 627–633 (2000).
87. Kanevsky, N. & Dascal, N. Regulation of maximal open probability is a separable function of Ca_vβ subunit in L-type Ca²⁺ channel, dependent on NH₂ terminus of α_{1C} (Ca_v1.2α). *J Gen Physiol* **128**, 15–36 (2006).

Acknowledgements

We thank Dr. Tatiana Ivanina and Dr. Vladimir Tsemakhovich for help with preparation of some of the DNA constructs and purified proteins, Reem Handklo and Boris Shalomov for help with a two electrode voltage clamp experiment, Mariam Ashkar for help with Western blots, and Drs Ilana Lotan, Moran Rubinstein and Daniel Yakubovich for critical reading of the manuscript. This work was supported by the USA-Israel Binational Science Foundation grant #2013/230, the Israel Science Foundation grant #1282/18, and the Mauerberger Chair for Neuropharmacology (N.D.).

Author Contributions

N.D., G.T. and U.K. conceived the study. N.D. and G.T. designed the study, planned the experiments, analyzed the data and wrote the manuscript. G.T. and T.K.R. carried out the experiments. All authors read and approved the final manuscript.

Additional Information

Supplementary information accompanies this paper at <https://doi.org/10.1038/s41598-018-36833-y>.

Competing Interests: The authors declare no competing interests.

Publisher's note: Springer Nature remains neutral with regard to jurisdictional claims in published maps and institutional affiliations.



Open Access This article is licensed under a Creative Commons Attribution 4.0 International License, which permits use, sharing, adaptation, distribution and reproduction in any medium or format, as long as you give appropriate credit to the original author(s) and the source, provide a link to the Creative Commons license, and indicate if changes were made. The images or other third party material in this article are included in the article's Creative Commons license, unless indicated otherwise in a credit line to the material. If material is not included in the article's Creative Commons license and your intended use is not permitted by statutory regulation or exceeds the permitted use, you will need to obtain permission directly from the copyright holder. To view a copy of this license, visit <http://creativecommons.org/licenses/by/4.0/>.

© The Author(s) 2019